



National Aeronautics and Space Administration

**Goddard Earth Science Data Information and
Services Center (GES DISC)**

ACOS Level 2 Standard Product and Lite Data Product Data User's Guide, v7.3

Revision Date: Revision F, January 12, 2017

**Goddard Space Flight Center
Greenbelt, Maryland**

**Jet Propulsion Laboratory
Pasadena, California**

Prepared By:

Gregory Osterman, JPL
ACOS, OCO-2 Science Validation Lead

Annmarie Eldering, JPL
OCO-2 Deputy Project Scientist

Cecilia Cheng, JPL
ACOS, OCO-2 Science Data Operations System

Christopher O'Dell, CSU
ACOS, OCO-2 Algorithms Team

David Crisp, JPL
OCO-2 Science Team Lead

Christian Frankenberg, JPL
ACOS, OCO-2 Algorithms Team

Brendan Fisher, JPL
ACOS, OCO-2 Validation Team

The work, recommendations and descriptions described in this document were carried out at the Jet Propulsion Laboratory, California Institute of Technology, under a contract with the National Aeronautics and Space Administration. Additional work was performed at the Colorado St University under the ACOS project.

© Copyright 2017. All Rights Reserved.

Revision History

| Revision Date | Changes | Author |
|------------------|--|--|
| 1 October 2010 | Initial Release | C. Avis |
| 20 December 2010 | Updates to most sections including changes to ACOS metadata/elements based on the v2.8.00 delivery. Updated quality provided by G.Osterman. | E. Martinez |
| 30 October 2011 | Complete revision of document. Includes updates for Build 2.9 | E. Martinez |
| 29 November 2011 | Rev B: Updated links to Mirador, corrected typos | E. Martinez |
| 7 December 2011 | Rev C: corrected typo on page 17 and added additional instructions on how to get data in section 4. ACOS release v2.9 | E. Martinez |
| 26 October 2012 | Rev D: Updated to further describe experience with v130130 data, and the preliminary experience with v15015x. Additional information about biases between Gain H and Gain M has been added. Errors associated with geolocation uncertainties also added. ACOS release v2.9 | D. Crisp |
| 29 October 2012 | Rev E: Updated for ACOS release v2.10 | C. O'Dell, G. Osterman, A. Eldering, D. Crisp, C. Avis |
| 15 April 2013 | Rev F: Updated for ACOS release v3.3 | C. O'Dell, G. Osterman, B. Fisher, C. Frankenberg, C. Avis |
| 3 October 2013 | Rev A: Updated for ACOS release v3.4 | C. O'Dell, G. Osterman, A. Eldering |
| 26 November 2013 | Rev B: Updated for version 3.4 release-2 | C. O'Dell, A. Eldering |
| 3 January 2014 | Rev C: Fixed minor typos and mistakes in bias-correction coefficients | C. O'Dell |
| 18 March 2014 | Rev D: Updated for version 3.4 release-3 | C. O'Dell |
| 14 July 2014 | Rev A : Updated for ACOS release v3.5 | C. O'Dell |
| 24 July 2014 | Rev B : Slight change to filtering and bias correction for v3.5 | C. O'Dell |
| 5 May 2015 | Rev C : Updated to release-2 bias correction for v3.5 | C, O'Dell |
| 28 March 2016 | Rev D : Minor updates to this guide to reflect latest literature and guidance, table updates to reflect v3.5 product | C. O'Dell, C. Avis G. Osterman |
| 12 January 2017 | Rev E: Updated for v7.3 release of the ACOS data product and description of the Lite data files | G. Osterman, A. Eldering, C. O'Dell |
| 19 October 2017 | Rev F: Fix a typo in the description of the XCO2 vs XCO2_raw fields | G. Osterman |

Table of Contents

| | |
|--|-----------|
| 1. INTRODUCTION | 1 |
| 1.1. SCOPE AND BACKGROUND | 1 |
| 1.2. OVERVIEW OF DOCUMENT | 1 |
| 1.3. DATA USAGE POLICY | 1 |
| 2. V7.3 ACOS L2 DATA PRODUCTS..... | 2 |
| 2.1. DIFFERENCES AMONG ACOS VERSIONS..... | 2 |
| 2.1.1. <i>Differences Between v3.5 and v7.....</i> | 2 |
| 2.2. VALIDATION STATUS | 2 |
| 2.3. DATA DESCRIPTION AND USER ALERTS | 2 |
| 2.4. DATA COMPLETENESS/COVERAGE..... | 2 |
| 2.5. CHLOROPHYLL FLUORESCENCE | 3 |
| 2.6. KEY SCIENCE DATA FIELDS..... | 5 |
| 2.6.1. <i>RetrievalResults/xco2.....</i> | 5 |
| 2.6.2. <i>SoundingHeader/cloud_flag</i> | 6 |
| 2.6.3. <i>RetrievalResults/surface_pressure_fph.....</i> | 6 |
| 2.7. SCIENCE ANALYSIS RECOMMENDATIONS | 6 |
| 2.7.1. <i>Differences among releases.....</i> | 6 |
| 2.7.2. <i>Recommended Data Screening</i> | 6 |
| 2.7.2.1. <i>Aerosol and cloud variables filter variables.....</i> | 7 |
| 2.7.2.2. <i>Other filter variables</i> | 8 |
| 2.7.3. <i>Recommended Bias Correction.....</i> | 9 |
| 2.7.3.1. <i>V7.3 (first release) bias correction (recommended).....</i> | 10 |
| 2.7.4. <i>Model-data comparisons and application to flux inversions.....</i> | 11 |
| 2.7.5. <i>GOSAT H- and M-Gain Data.....</i> | 12 |
| 3. BACKGROUND READING | 12 |
| 3.1. ABOUT THE GOSAT MISSION | 12 |
| 3.1.1. <i>Instrument.....</i> | 13 |
| 3.1.2. <i>Orbital Parameters</i> | 13 |
| 3.1.3. <i>Path ID Definition.....</i> | 14 |
| 3.2. GOSAT L1B RELEASES | 14 |
| 3.3. ABOUT THE ACOS TASK..... | 14 |
| 3.4. ACOS ALGORITHMS..... | 16 |
| 3.4.1. <i>Level 1B Algorithm Overview</i> | 16 |
| 3.4.2. <i>Level 2 Algorithm Overview</i> | 17 |
| 3.5. ACOS DATA PRODUCTS..... | 18 |
| 3.5.1. <i>File Naming Convention.....</i> | 18 |
| 3.5.2. <i>File Format and Structure</i> | 19 |
| 3.5.3. <i>Data Definition.....</i> | 19 |
| 3.5.4. <i>Global Attributes</i> | 20 |
| 3.5.5. <i>ACOS Metadata and Variables</i> | 21 |
| 4. ACOS LEVEL 2 LITE DATA PRODUCTS | 37 |
| 5. TOOLS AND DATA SERVICES..... | 40 |
| 6. CONTACT INFORMATION..... | 42 |
| 7. ACKNOWLEDGEMENTS, REFERENCES AND DOCUMENTATION | 43 |

Table of Figures

| | |
|--|----|
| Figure 1: Monthly maps of the ACOS v7.3 X_{CO_2} data. Each data point contains the average value for X_{CO_2} estimates in a $2^\circ \times 2^\circ$ bin for that month that passed all pre- and post-screening filters; the recommend bias correction has been applied..... | 4 |
| Figure 2: Plot showing the land gain H filtering process, without (black) and with (light blue) bias correction. Each panel shows the mean bias of the retrieved X_{CO_2} as evaluated against TCCON for the v7.3 dataset. The figure should be read left-to-right, top-to-bottom. Each panel shows the effect of a filter variable, applied cumulatively to all the variables that came before it. In the top right corner of each panel is displayed the number of surviving soundings after that filter has been applied (again, cumulatively), and the standard deviation of the X_{CO_2} errors for those soundings surviving to that point. The dark blue diamonds show the standard deviation of the X_{CO_2} error in each bin. | 9 |
| Figure 3: GOSAT Observation Concept..... | 13 |
| Figure 4: GOSAT TANSO-FTS Observation Details..... | 14 |
| Figure 5: Level 2 Full Physics Retrieval Flow..... | 18 |

Table of Tables

| | |
|--|----|
| Table 1: Screening criteria for v7.3 level-2 XCO ₂ retrievals | 6 |
| Table 2: v7.3 bias correction parameters and their estimated uncertainties. | 11 |
| Table 3: Description of the different GOSAT L1B releases..... | 15 |
| Table 4: Some Global Metadata Attributes | 20 |
| Table 5: Key Metadata Items | 20 |
| Table 6: Metadata Information | 21 |
| Table 7: Spacecraft Geometry Variables | 23 |
| Table 8: Sounding Geometry Variables..... | 24 |
| Table 9: Sounding Header Variables | 25 |
| Table 10: A-Band-only Retrieval Variables | 25 |
| Table 11: IMAP-DOAS Retrieval Variables..... | 26 |
| Table 12: Retrieval Header Variables | 27 |
| Table 13: Variables Expressing Retrieval Results..... | 28 |
| Table 14: Spectral Parameter Variables | 35 |
| Table 15: Bit Flag Definitions | 35 |
| Table 16 provides a description of the fields in the ACOS Lite Data Product files..... | 37 |
| Table 17 Contains description of the fields in the “Preprocessor” folder of the Lite files. | 38 |
| Table 18 Contains description of the fields in the “Retrievals” folder of the Lite files. | 38 |
| Table 19 Contains description of the fields in the “Sounding” folder of the Lite files. | 39 |

1. Introduction

1.1. Scope and Background

This document provides an overview of the v7.3 (sometimes called B7, or B7.3; they are all the same). Atmospheric CO₂ Observations from Space (ACOS) data product, key features and issues, preliminary validation information, recommendations on data usage, as well as background on the Greenhouse Gases Observing Satellite (GOSAT) mission measurements and the ACOS algorithm. The later sections provide the reader with information on filename conventions and a detailed guide to the format and fields in the hdf product.

This is the seventh 'public release' of ACOS data, the previous released version being v3.5, which was released in August 2014. The ACOS v2.10 data were unofficially released in October 2012. The v2.8 and v2.9 data are described in a series of validation papers published in 2011 and 2012. This document updates findings from these papers for v7.3, and gives more general information on the use of ACOS data.

While Build 7 is now relatively mature, the Build 7 (v7.3) retrievals continue to be evaluated, and the guidance provided herein may be incomplete. Version 7.3 is the latest version of the ACOS data to be released after the launch of the Orbiting Carbon Observatory-2 (OCO-2) in July 2014. The retrieval algorithm used to create the Build 7 ACOS data product is consistent with that used to create the OCO-2 v7.3 data product. This will allow comparison of the ACOS and OCO-2 data without having to consider algorithm differences.

1.2. Overview of Document

The remainder of this section describes the usage of the ACOS data. Section 2 provides details of the differences in this version, product characteristics, validation status, key data fields and ends with recommendations for data analysis. Section 3 provides background information on the GOSAT mission, ACOS file and data conventions, and a complete listing of metadata elements in the v7.3 ACOS data product. Section 4 lists tools to view and search the data products. Section 5 lists contact information for both GOSAT and ACOS data, and the last section lists acknowledgements and relevant publications.

1.3. Data Usage Policy

This data has been produced by the ACOS project, and is provided freely to the public. The ACOS project has been made possible by the generous collaboration with our Japanese colleagues at Japanese Aerospace Agency (JAXA), National Institute for Environmental Studies (NIES), and the Ministry of the Environment (MOE). The Level 1 GOSAT data have been made available for this project through an agreement between the GOSAT Three Parties and Caltech. In order to improve our product and receive continued support for this work, we need user feedback and also have users properly acknowledge data usage. Therefore, we request that when publishing using ACOS data; please acknowledge NASA and the ACOS/OCO-2 project.

- Include OCO-2 as a keyword to facilitate subsequent searches of bibliographic databases if it is a significant part of the publication
- Include a bibliographic citation for ACOS/OCO-2 data. The most relevant citations currently are Wunch et al (2011), O'Dell et al (2012) and Crisp et al. (2012).

- Include the following acknowledgements: "These data were produced by the ACOS/OCO-2 project at the Jet Propulsion Laboratory, California Institute of Technology, and obtained from the JPL website, co2.jpl.nasa.gov."
- Include an acknowledgement to the GOSAT Project for acquiring these spectra.
- We recommend sending courtesy copies of publications to the OCO-2 Project Scientist, Michael.R.Gunson@jpl.nasa.gov.

2. V7.3 ACOS L2 Data Products

2.1. Differences among ACOS versions

2.1.1. Differences Between v3.5 and v7

Changes to the L2 products are as follows:

- Changes to input or ancillary data used to process the L2 products
 - New versions of the GOSAT L1B data. From April 2009 through March 2016, v201201 of the L1B data was used. April 2016 onward uses v201202.
- Within the code (many of these changes make the code used for ACOS data processing consistent with that used for OCO-2)
 - Surface pressure a priori constraint is ± 2 hPa (v3.5 used ± 1 hPa)
 - Updated cloud ice properties, now consistent with MODIS collection 6.
 - The number of EOFs used was 3 (v3.5 used 1)
 - Updates to bias correction and screening recommendations

2.2. Validation Status

The v7.3 ACOS X_{CO_2} data product has undergone a *preliminary* validation against both TCCON data and atmospheric models. Detailed comparisons of previous ACOS versions to TCCON have been published in Wunch et al. (2011b), Lindqvist et al. (2015) and Kulawik et al. (2016). More work is being done to inter-compare the ACOS v7.3, OCO-2 v7.0 and TCCON data.

2.3. Data Description and User Alerts

There are some differences between the results from ACOS software v7.3 and those from previous builds. In previous data versions there were retrievals for both GOSAT High (H) gain and Medium (M) gain, as well as ocean glint data (virtually all of which is taken in High gain). ACOS B7 ONLY contains high gain; medium gain has not yet been bias corrected, and so is not included in the lite files. Both gains are included in the (larger) standard files, but users should beware that there is not formally recommended filtering or bias correction for gain M soundings.

2.4. Data Completeness/Coverage

- GOSAT L1B Version 201201 was used for all L2 retrievals in v7.
- The first three months of GOSAT operations (April-May, 2009) have incomplete operational coverage due to on-orbit calibrations and checkout activities. Full coverage begins about 1 July 2009. Users should exercise caution when using any data before 1 July 2009.

- Typically, data products contain 10-100 useful soundings per orbit, out of the 600-700 L1B soundings collected in an orbit. Note that over 50% of the data is not processed because it does not pass the first cloud screening pre-processing step. A large fraction of data is collected over ocean but not in glint, and thus is not processed. Of the ~100 soundings that are processed for each orbit, convergence and quality screens identify about 50% of that data as good.
- If data users create maps of the filtered v7.3 carbon dioxide data, they should expect to see glint measurements move north and south during the year. Figure 1 shows maps from ACOS v7.3 data, illustrating how the glint observations change with time of year.

2.5. Chlorophyll Fluorescence

Since ACOS v3.3, solar-induced chlorophyll fluorescence (SIF) is included in the full-physics code as an additional state vector element. This is true for v7.3 as well and the main motivation for this is to reduce a potential bias on XCO_2 , as outlined in detail in Frankenberg et al. (2012). This product, however, should not be used to look at chlorophyll fluorescence itself, as there is a high interference with other state vector elements (surface pressure, albedo, aerosols). Fluorescence is NOT fit for in gain M data over land, which is primary non-vegetated desert, as well as ocean data, where the ocean fluorescence signal from phytoplankton is expected to be small. The SIF product included in the ACOS data products should not be used

The IMAP-DOAS preprocessor performs fluorescence retrievals using Fraunhofer lines only, which is more robust and should be used as the ACOS fluorescence product. However, the fields reported in the official level 2 file have not yet been optimally corrected for the 0-level offset observed in GOSAT O_2 A-band spectra (Frankenberg et al, 2011). A separate unofficial fluorescence dataset (monthly ascii files of single soundings) will be available upon request (contact is Christian Frankenberg cfranken@caltech.edu).

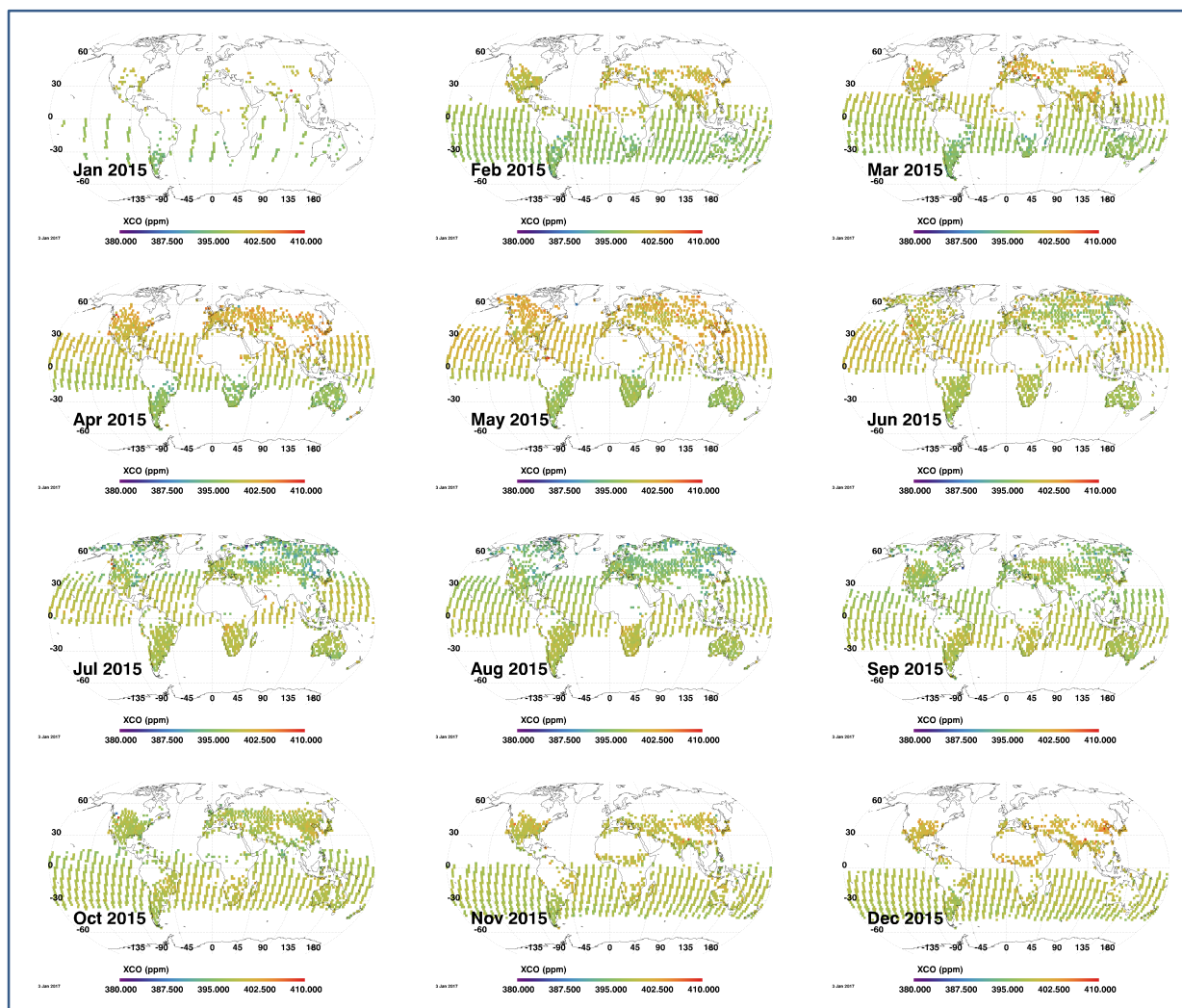


Figure 1: Monthly maps of the ACOS v7.3 X_{CO_2} data. Each data point contains the average value for X_{CO_2} estimates in a $2^\circ \times 2^\circ$ bin for that month that passed all pre- and post-screening filters; the recommend bias correction has been applied.

Cloud-Screening

- To further reduce the computation time of retrievals containing clouds, the cloud screening algorithm is applied to this version. It performs a fast, Oxygen A-band only clear-sky retrieval for surface pressure, surface albedo, temperature offset and dispersion multiplier. The retrieved surface pressure and albedo information are combined with the χ^2 goodness-of-fit statistic and signal-to-noise ratio to determine if a scene is clear(0), cloudy (1), or skipped (2). The difference of this retrieved surface pressure with respect to the prior ECMWF analysis-based estimate serves as the chief filter criterion; this difference must be less than 25 hPa for the sounding to pass the screen. See Taylor et al. (2012) for further details on the Oxygen A-band cloud-screening algorithm.

Pre-Processing for v7

The v7.3 preprocessing is the same as that for version v3.5. In version v3.5, a preprocessing scheme was used that is similar to that used for the v3.3 (and earlier) ACOS data version. This is in contrast to v3.4, which used additional pre-filters to speed up processing. This additional processing speed was not necessary for v7.3, so only a mild cloud-screen was used (see above). In the case of soundings over water, a check was made to ensure the observation was made in glint mode.

Post-Processing

- No bias correction – the retrieval results in the standard HDF files have not been systematically corrected based upon some known reference source. Bias corrected XCO₂ values are provided in the ACOS v7.3 “Lite” files.
- No post-screening – the results in the standard HDF files include all soundings whose retrieval did not crash or exit with an error status. This means that even some non-converged soundings are present in the standard HDF files.
- No post-processing filter has been applied to eliminate soundings based upon certain criteria.

Quality Flagging

- There are several quality flags among the variables. The user should weigh the following information about the flags:
 - *Retrieval_header/sounding_qual_flag* – quality of input data provided to the retrieval processing
 - *Retrieval_results/outcome_flag* – retrieval quality based upon certain internal thresholds, which mainly describes where a sounding converged (*outcome_flag* = 1 or 2), or failed to converge (*outcome_flag* = 3 or 4).

Averaging Kernels

- The data files include a column averaging kernel value for each retrieved sounding.
- The normalized Averaging Kernel (*retrieval_results/xco2_avg_kernel_norm*) for a given pressure level is equal to the non-normalized value (*retrieval_results/xco2_avg_kernel*) divided by the pressure weighting function at that level. Note that levels are “layer boundaries” and have no thickness.

Known Problems

- Pointers to other files (e.g., ‘*InputPointer*’) are not useful because those files reside only on the originating system and were not delivered to the GES DISC.

2.6. Key Science Data Fields

2.6.1. RetrievalResults/xco2

The Level 2 Standard Product contains the variable XCO₂. This variable expresses the column-averaged CO₂ dry air mole fraction for a sounding. These values are determined by a full-physics retrieval and have units of mol/mol.

2.6.2. SoundingHeader/cloud_flag

The Level 2 Standard Product contains the variable *cloud_flag*. This variable expresses the result of an analysis of cloud contamination within a sounding. Every sounding of a granule will have a value: 0 (Clear), 1 (Cloudy) or 2 (Undetermined). The values are determined by an ABO2-band-only retrieval using the FTS spectrum. The only soundings that will be processed by the L2 software are those with a value of 0 (Clear). However, this does NOT mean that all processed soundings are actually clear. Some cloudy scenes are invariably missed by the ABO2-only preprocessor, but can lead to bad XCO₂ retrievals. Therefore, users are strongly encouraged to further apply the recommended quality filters given in section 2.7.2.

2.6.3. RetrievalResults/surface_pressure_fph

The Level 2 Standard Product contains the variable *surface_pressure_fph*. This variable expresses the retrieved atmospheric pressure at the Earth's surface for a given sounding. Those soundings that did not converge will not be present. These values are determined by a full-physics retrieval and have units of Pascals.

2.7. Science Analysis Recommendations

2.7.1. Differences among releases

This represents the first release of the filtering and bias correction for the v7.3 retrievals. The filters are similar but not identical to those users for the previous version, v3.5

2.7.2. Recommended Data Screening

We now describe the recommended filters for science data screening. Good soundings will be those that pass all the criteria in Table 1. Note that these screenings, while similar, are distinctly different from that of v3.5. Therefore the screening for v7.3 should be used on v7.3 retrievals, and v3.5 screening only used on v3.5 retrievals.

Table 1: Screening criteria for v7.3 level-2 XCO₂ retrievals

| Variable | Ocean Glint | Land H |
|--|---------------|----------------|
| RetrievalResults/outcome_flag | 1 or 2 | 1 or 2 |
| RetrievalResults/aerosol_total_aod | < 0.5 | 0.04 to 0.3 |
| AOD Sulfate | | <0.2 |
| OD_Ice_cloud | | 0.0013 to 0.07 |
| Ice_Height | < 0.5 | -0.2 to 0.475 |
| IMAPDOASPreprocessing/co2_ratio_idp | | 0.99 to 1.017 |
| IMAPDOASPreprocessing/h2o_ratio_idp | | 0.85 to 1.04 |
| $\Delta P_{s, \text{cld}}$ [hPa] | | -13.0 to 3.0 |
| RetrievalResults/xco2_uncert • 10 ⁶ [ppm] | | < 1.7 |
| SoundingGeometry/sounding_altitude | | < 2500 |
| SpectralParameters/signal_weak_co2_fph | | < 7.8e-7 |
| RetrievalResults/albedo_slope_o2 • 10 ⁵ | | -5.0 to 1.0 |
| $\Delta Grad_{CO_2}$ [ppm] | -22.0 to 12.0 | -25 to 125 |

| Variable | | |
|--|-------------|-------------|
| RetrievalResults/albedo_strong_co2_fph | | 0.0 to 0.4 |
| ΔP_s [hPa] | -1.0 to 5.5 | -7.0 to 7.0 |
| RetrievalResults/albedo_slope_strong_co2 • 10 ⁵ | > -2.0 | |
| RetrievalResults/albedo_slope_weak_co2 • 10 ⁵ | < 2.0 | |
| SpectralParameters/reduced_chi_squared_strong_co2_fph | < 1.35 | |

Some variables in the table must be constructed directly by users of the standard L2s HDF-5 files. All these variables should appear directly in the “Lite” files.

2.7.2.1. Aerosol and cloud variables filter variables

Because of the new variable aerosol types retrieved, extracting the amount of optical depth in each species is a bit trickier than in previous versions. For each sounding, there are four species of scatterers retrieved:

1. Aerosol type 1. May be type dust (DU), sulfate (SO), OC (Organic Carbon), black carbon (BC), or sea salt (SS).
2. Aerosol type 2. May be DU, SO, OC, BC, or SS, and will be different from aerosol type 1.
3. Ice cloud
4. Water cloud

The HDF-5 files specify the fitted AOD and height for each species in terms of their number (1-4). Additionally, the variable “*RetrievalResults/aerosol_types*” indicates which type each aerosol corresponds to for a given sounding.

The following variables can then be constructed for use in the filtering. Some may also be needed for the bias correction.

- **AOD_Sulfate.** Find each sounding for which “aerosol_types” equals “SO”. For each such sounding, the AOD due to sulfate is simply “RetrievalResults/aerosol_X_aod”, where X is either type 1 or 2.
- **AOD_Dust.** As for *AOD_Sulfate*, but the AOD where “aerosol_types” equals “DU”.
- **AOD_SeaSalt.** As for *AOD_Sulfate*, but the AOD where “aerosol_types” equals “SS”.
- **AOD_Water_cloud** Because Water cloud is always retrieved, and it always occurs as type 4 in version v7, the retrieval optical depth (OD) due to Water cloud is simply:

$$OD_Water_Cloud = RetrievalResults/aerosol_4_aod$$

- **OD_Ice_cloud.** Because Ice cloud is always retrieved, and it always occurs as type 3 in version v7, the retrieval optical depth (OD) due to Ice cloud is simply:

$$OD_Ice_Cloud = RetrievalResults/aerosol_3_aod$$

- **Ice_Height** is the central pressure location of the retrieved ice cloud type, relative to the surface pressure. It has values typically between 0 and 1, though it can go slightly negative. It is the **second** element of the vector:

$$\text{Ice_Height} = \text{RetrievalResults/aerosol_3_gaussian_log_param}$$

2.7.2.2. Other filter variables

- ΔP_s is the difference of the retrieved and prior surface pressure, given in hPa. It is constructed as

$$\Delta P_s = (P_{s,\text{retrieved}} - P_{s,\text{prior}}) * 0.01$$

where $P_{s,\text{retrieved}}$ is the retrieved surface pressure

RetrievalResults/surface_pressure_fph and $P_{s,\text{prior}}$ is the prior (meteorological) surface pressure from ECMWF (*RetrievalResults/surface_pressure_apriori_fph*).

- $\Delta P_{s,\text{cld}}$ is the difference of the retrieved and prior surface pressure from the A-band cloud-screen, expressed in hPa:

$$\Delta P_{s,\text{cld}} = \text{ABandCloudScreen/surface_pressure_delta_cloud} \cdot 0.01$$

- **Grad_{CO2}** is the difference in retrieved CO2 dry-air mole fraction between the surface and vertical level 13. Vertical level 13 is the level with $P/P_{\text{surf}} = 12/19 = 0.631579$. This is about 630 hPa for sounding elevations near sea level. This variable is something like a “lapse rate for CO2”. High positive or negative values of this variable are indicative of poor soundings.
- **ΔGrad_{CO2}** is the change in **Grad_{CO2}** for the retrieved value with respect to the *a priori* value. It is essentially how much the “lapse rate for CO2” has changed from the prior value to the retrieved value, and also can be indicative of bad soundings. The CO₂ profile for the prior is stored in *RetrievalResults/co2_profile_apriori*, and the retrieved profile is stored in *RetrievalResults/co2_profile*.
- **DWS** is the sum of the retrieved optical depths of Dust, Water cloud, and Sea Salt. From the definitions given above, it is then:

$$\text{DWS} = \text{AOD_Dust} + \text{AOD_SeaSalt} + \text{OD_Water_cloud}$$

Figure 2 illustrates the filtering process for land, gain H ACOS data.

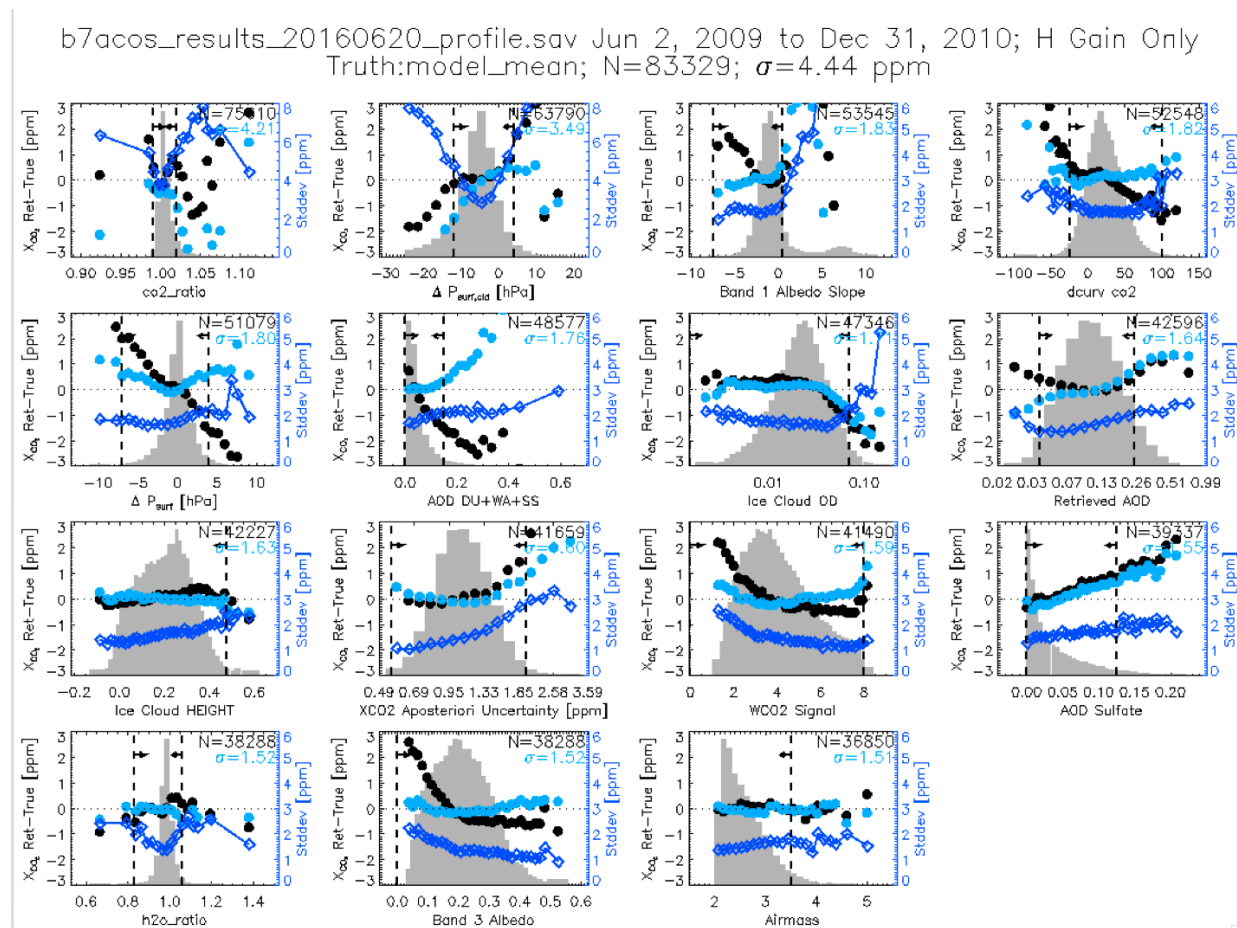


Figure 2: Plot showing the land gain H filtering process, without (black) and with (light blue) bias correction. Each panel shows the mean bias of the retrieved X_{CO_2} as evaluated against TCCON for the v7.3 dataset. The figure should be read left-to-right, top-to-bottom. Each panel shows the effect of a filter variable, applied cumulatively to all the variables that came before it. In the top right corner of each panel is displayed the number of surviving soundings after that filter has been applied (again, cumulatively), and the standard deviation of the X_{CO_2} errors for those soundings surviving to that point. The dark blue diamonds show the standard deviation of the X_{CO_2} error in each bin.

2.7.3. Recommended Bias Correction

In addition to a global bias, errors in the X_{CO_2} retrievals have been found to correlate well with certain other variables. This has been true in all previous versions of the algorithm. This issue was first explored for B2.8 and B2.9 (Wunch et al., 2011), in which four regression variables were used to correct ACOS (land, gain H) data. No correction was given for land gain M or ocean glint data at that time. This procedure was expanded in the B2.10 retrievals to also include land gain M and ocean glint soundings. There, two variables were used to bias-correct land soundings, and three were used for ocean soundings. The same methodology was followed in v3.3 for land gain H data only (as land gain M and ocean data were not trustworthy from this

version), and a two-parameter bias-correction was found there. A similar procedure was followed for v3.4 for all 3 modes (land gain H, land gain M, ocean glint).

For v3.5 and v7.3 retrievals, we again follow the same methodology but again arrive at slightly different bias-correcting variables and coefficients as compared to previous versions. This is due to the changes in the algorithm, primarily due to the new aerosol treatment. For the bias correction formulae given below, there is some uncertainty in the fit coefficients as well as the overall mean bias. We estimate these uncertainties for each parameter and mean bias term, as rough 1-sigma uncertainties. These may be incorporated into inversion systems to formally account for these uncertainties. The uncertainties were obtained by using both models and TCCON as validation data sources, and the differences in the fit coefficients were used as a rough proxy for uncertainty.

As mentioned above, a similar procedure was followed for v7.3, but due to time constraints alone, it was not done for gain M. This could be changed in the future, if there is significant interest in the community for doing so.

The following bias correction formulae have been derived separately for land gain H and ocean glint. All formulae were derived using multiple linear regression to both TCCON, version ggg2014, and model data. Mean bias terms were estimated solely from TCCON (version ggg2014). Coefficient values and their parameters are given in Table 2.

2.7.3.1. V7.3 (first release) bias correction (recommended)

In units of ppm, the X_{CO2} bias correction formulae are as follows.

Land Gain H

$$\begin{aligned} X_{CO2}' = & X_{CO2} + 0.15 \\ & + 0.30 (\Delta P_s) \\ & + 8.6 (\sqrt{\alpha_3} - 0.5) \\ & + 0.016 (\Delta Grad_{CO2} - 25) \\ & + 14.5 (DWS - 0.02) \end{aligned}$$

Ocean Glint

$$\begin{aligned} X_{CO2}' = & X_{CO2} + 0.9 \\ & - 42.4 (S_{32} - 0.61) \\ & - 0.093 (\Delta Grad_{CO2} + 3.0) \\ & + 1.8 (\underline{Ice\ Height} - 0.18) \\ & + \underline{0.325} (\underline{logDust}) \end{aligned}$$

where α_3 is the retrieved albedo in Band 3 (*RetrievalResults/albedo_strong_co2_fph*). We have found that for this version, the bias is almost linear in the square root of α_3 , so have adopted it directly into the v7.3 bias correction. *logDust* is the natural logarithm of the AOD_Dust (defined in the previous section). S_{32} is the ratio of signal in band 3 to the signal in band 2 (*SpectralParameters/signal_strong_co2_fph / SpectralParameters/signal_weak_co2_fph*). All other variables were defined in the preceding section.

Some users may wish to have information regarding the uncertainty in the bias correction. This is difficult to quantify for a number of reasons. First, the validation data source (such as TCCON or the SH Approximation as used in Wunch et al., 2011) each have their own uncertainties and limitations. Training the bias correction separately on each generally results in slightly different fit coefficients. Second, the ACOS soundings themselves have errors, and incorporating all these error sources into a robust parameterization of the bias correction error is nontrivial. Therefore, the uncertainties given in Table 2 are only rough estimates, based loosely on the above considerations.

Table 2: v7.3 bias correction parameters and their estimated uncertainties.

| Bias Correction Parameters | Value \pm Uncertainty (1σ) |
|----------------------------------|---------------------------------------|
| Land Gain H | |
| ΔP_5 Coefficient | -0.3 ± 0.02 |
| $\sqrt{\alpha_3}$ Coefficient | -8.6 ± 1.0 |
| $\Delta Grad_{CO_2}$ Coefficient | -0.016 ± 0.002 |
| DWS Coefficient | -14.5 ± 1.0 |
| Mean Bias [ppm] | -0.15 ± 0.25 |
| Ocean Glint | |
| S_{32} Coefficient | 42.4 ± 2 |
| $logDust$ Coefficient | -0.325 ± 0.05 |
| $\Delta Grad_{CO_2}$ Coefficient | 0.093 ± 0.015 |
| Ice_Height Coefficient | -1.8 ± 0.3 |
| Mean Bias [ppm] | -0.9 ± 0.25 |

2.7.4. Model-data comparisons and application to flux inversions

When comparing the ACOS XCO₂ to models, it is recommended to make use of our column averaging kernel. The ACOS level-2 retrieval first retrieves a profile of CO₂ dry-air mole fraction on twenty layer boundaries. The lowest pressure boundary is at the surface. XCO₂ given as:

$$X_{CO_2} = \mathbf{h} \cdot \mathbf{u} \quad (2.6)$$

where \mathbf{h} is the pressure weighting function vector and \mathbf{u} is the retrieved vector of CO₂ dry air mole fraction. In theory, we retrieve a weighted average of the true profile and our prior profile, plus a contribution from measurement noise:

$$\mathbf{u} = \mathbf{A}\mathbf{u}_{true} + (\mathbf{I} - \mathbf{A})\mathbf{u}_{ap} + \mathbf{G}\boldsymbol{\varepsilon} \quad (2.7)$$

where \mathbf{A} is the full averaging kernel matrix, \mathbf{u}_{true} is the true profile of CO₂, \mathbf{u}_{ap} is the prior profile of CO₂ used by the L2 code, \mathbf{G} is the retrieval gain matrix, and $\boldsymbol{\varepsilon}$ is measurement noise. Hitting this equation with the pressure weighting function on the left, we arrive at a simple equation for our retrieved XCO₂:

$$X_{CO_2} = \mathbf{a} \cdot \mathbf{u}_{true} + (\mathbf{h} - \mathbf{a}) \cdot \mathbf{u}_{ap} + (\mathbf{h}'\mathbf{G}) \cdot \boldsymbol{\varepsilon} \quad (2.8)$$

where \mathbf{a} is called the (un-normalized) column averaging kernel. When comparing to models, it is useful to form the normalized column averaging kernel \mathbf{a}_{norm} , where

$$\mathbf{a}_{norm,i} = \mathbf{a}_i / \mathbf{h}_i \quad (2.9)$$

for each of our 20 levels i . When comparing model X_{CO_2} to measured, one should interpolate the model CO_2 profile to the ACOS pressure grid, and call that the truth in equation 2.8 (and setting the noise term to zero). \mathbf{h} and \mathbf{a} are both given in the data files. The vertical grid in the level-2 retrieval algorithm is a sigma pressure grid, such that the pressure at level i is given by

$$P_i = b_i P_{surf} \quad (2.9)$$

Here, P_{surf} is the retrieved surface pressure and b is vector of 20 coefficients (one for each vertical level). This is called “SigmaB” in the ACOS Lite product file. For versions after v3.4, this vector is $\mathbf{b}=(1e-4, 1/19, 2/19, \dots, 18/19, 1.0)$.

For users need the full state vector averaging kernel and/or covariances matrices, these are available upon request (please email Christopher.ODell@colostate.edu).

2.7.5. GOSAT H- and M-Gain Data

The TANSO-FTS on the GOSAT satellite makes measurements in different modes. The different gain modes appear to suffer from slightly different biases, and the bias correction described above attempts to correction for these differences. Therefore, users should recognize that these differences exist, and while there is a bias-correction, it is not perfect and it is important to recognize that there may be residual differences in X_{CO_2} errors between these modes.

The gain setting can be determined by looking at the “RetrievalHeader/gain_swir” variable in the ACOS data product. Note that this variable has two character string entries per sounding – one for the S polarization and one for the P polarization. For ACOS retrievals, P & S polarizations have been averaged together to produce an approximation of the total intensity I .

Finally, as a reminder post-retrieval filtering and bias correction was not performed for any gain M retrievals (which nearly always occur over bright surfaces over land). This was done purely due to time constraints. Raw, unfiltered gain M soundings do appear in the standard products, but do not appear in the Lite products due to this reason. Any gain M soundings pulled from the standard product should be used with caution (users will need to attempt their own filtering and bias correction in this case).

3. Background Reading

3.1. About the GOSAT Mission

The Japanese GOSAT mission was successfully launched on January 23, 2009. The GOSAT prime mission extends five years from the date it was declared operational on April 19, 2009.

3.1.1. Instrument

The primary GOSAT science instrument is the Thermal And Near infrared Sensor for carbon Observation (TANSO). It is a Fourier-Transform Spectrometer (FTS) with 2-axis scanner. The scanner directs light into two sets of detectors within the instrument.

The Short Wave InfraRed (SWIR) detector is designed to measure the spectrum of reflected sunlight from both land and water surfaces. Three spectral regions are covered in two polarizations:

| | | |
|--------|---------------------------|--------------------------------------|
| Band 1 | .75 - .78 μm | Oxygen, a.k.a. ABO2 |
| Band 2 | 1.56 – 1.72 μm | Weak CO ₂ , a.k.a. WCO2 |
| Band 3 | 1.92 – 2.08 μm | Strong CO ₂ , a.k.a. SCO2 |

The Thermal InfraRed (TIR) detector is designed to measure the spectrum of thermal radiation from both land and water surfaces. A single spectral region is covered (5.5 – 14.3 μm). The ACOS Level 2 products do not include or utilize any TIR data.

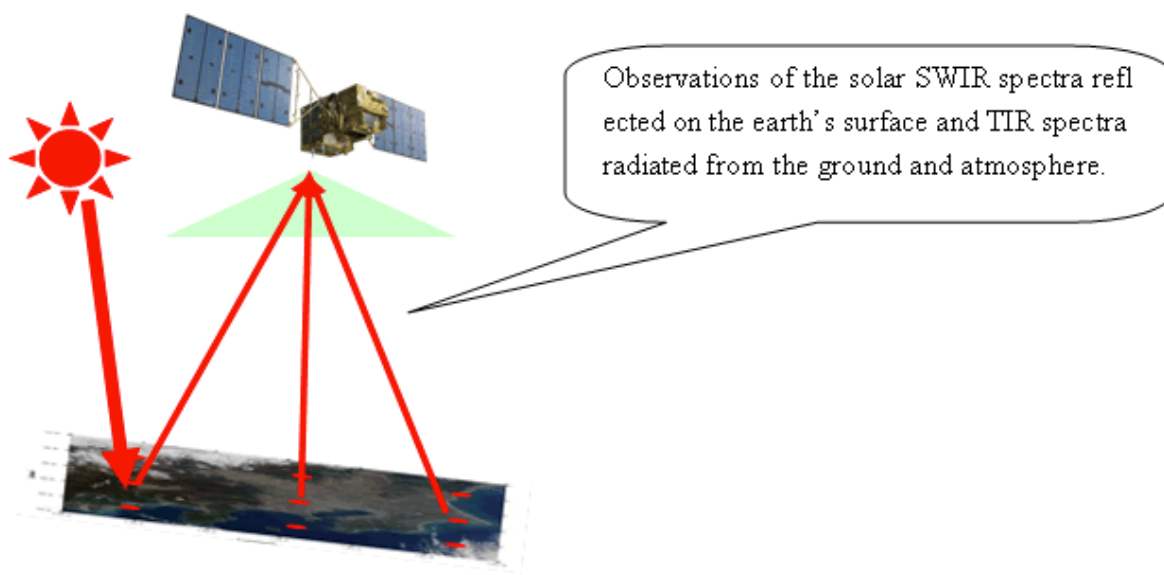


Figure 3: GOSAT Observation Concept

3.1.2. Orbital Parameters

GOSAT nominal orbit parameters are shown below.

- Orbit Type: sun-synchronous, ground track repeat, near-circular orbit
- Recurrent period: 3 days
- Recurrent orbit number: 44
- Revolutions per day: 14+2/3 rev/day
- Local sun time at descending node: 12:45 – 13:15 PM
- Altitude above equator: 665.96 km
- Orbital Period: 98.1 minutes
- Inclination: 98.06 degrees
- Eccentricity: 0.0 (Frozen orbit)

- Longitude at ascending node: Longitude 4.92 degrees west for orbit 1
- Footprint size on ground: 10.5 km circle when NADIR viewing

3.1.3. Path ID Definition

The Path ID identifies the GOSAT orbit tracks on the ground. The detailed characteristics are as follows:

- A path begins at ascending node and extends to the next ascending node
- The ascending node of the Path with an ID of 1 is at longitude 4.92 degrees west
- The path number of the orbit tracks westward sequentially
- Path IDs run from 1 through 44
- Path calculator: https://data.gosat.nies.go.jp/map/html_E/MapPathCalendar.html

Note that Figure 4 illustrates 5-point sampling, which was used from April 2009 through July of 2010. Since August of 2010, a 3-point sampling mode has been used.

| Points | Interval |
|----------------|----------|
| 1 | 789 km |
| 3 | 263km |
| 5 (nominal) | 158km |
| 7 | 113km |
| 9 | 88km |

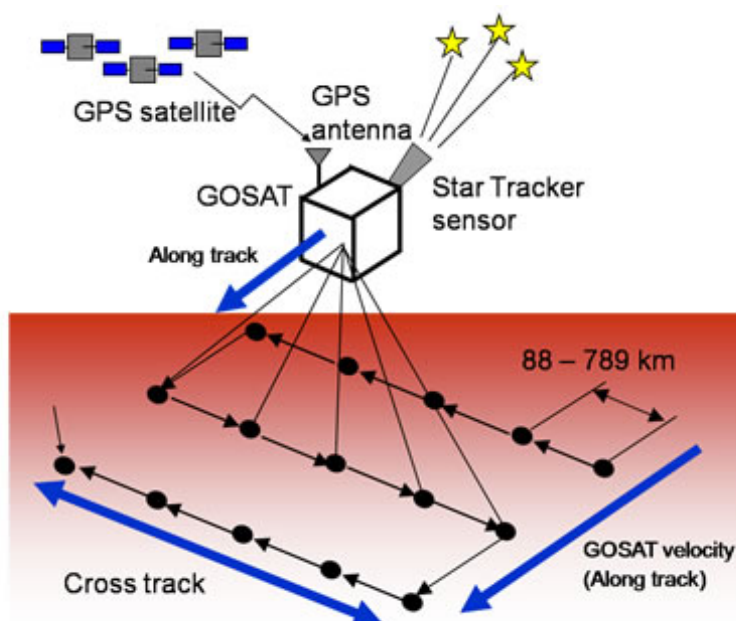


Figure 4: GOSAT TANSO-FTS Observation Details

3.2. GOSAT L1B Releases

The L1B radiance data are provided to the ACOS project by JAXA. As instrument characteristics are better understood, there have been some changes to the L1B data. Table 3 provides a high level view of the L1B versions and key characteristics. Section 3.5.1 shows how the L1B version that was used can be identified in the L2 product file name.

3.3. About the ACOS Task

The ACOS project is part of the Earth System Science Pathfinder (ESSP) Program in the NASA Science Mission Directorate (SMD). The Orbiting Carbon Observatory (OCO) was to have been the first NASA satellite designed to make global measurements of atmospheric carbon dioxide

(CO₂) sources and sinks on regional scales at monthly intervals. The failure of the launch system and loss of the observatory therefore represented a setback to NASA's carbon cycle and climate science programs.

To meet its stringent CO₂ measurement accuracy requirements, the OCO Science Team developed and implemented several significant advances in ground-based calibration, validation, and remote sensing retrieval methods. These investments were not lost in the OCO launch failure and remain valuable NASA assets.

The OCO and GOSAT Science Teams formed a close partnership in calibration and validation activities. JAXA granted the ACOS Project access to GOSAT's calibrated Level 1B measurements. The ACOS Project applies the OCO calibration, validation, and remote sensing retrieval assets to analyze these GOSAT measurements. These analyses generate the Level 2 data products described herein.

Table 3: Description of the different GOSAT L1B releases.

| Version | Period YYMMDD | Changes |
|-------------------|--|---|
| Version006006 (P) | 090423–090504 090516–090728 | <ul style="list-style-type: none"> initial version |
| Version007007 (P) | 090405–090409 090419–090429 090716–091029 | <ul style="list-style-type: none"> SWIR spectrum unit is changed: (V -> V/cm-1) SWIR phase correction parameter is changed. (Gauss function parameter; 0.060000 -> 0.002000, see "TANSO Level 1Product Description Document" page 3-29) Orbital data is changed. (predicted value -> fixed value) Threshold of sun-glint cone angle is changed. (10 degrees -> 5 degrees) New product items are added. |
| Version050050 | 090405–090409 090419–090503 090602–090731 091028–100208 | <ul style="list-style-type: none"> TIR phase correction (ZPD shift) New item on spike noise judgment is added. Threshold of saturation flag is changed. Low-frequency correction. flag judgment is improved. |
| Version080080 | 090731–091001 100208–100316 | <ul style="list-style-type: none"> Calibration formula of TIR radiance spectrum are added. (But parameters are modified so that radiance values remain the same as those for V050.) The accuracy of SWIR spike flag judgment is improved. "CT_obsPoints" value is changed to "0X0a", when sensor mode is "specific point observation". As a result, it can be distinguished from the case of sensor anomaly. AT/CT error angles are expressed in GOSAT/TANSO sensor coordinate. Orbit and attitude parameters are changed. |
| Version100100 | 090930–091031 100315–110419 | <ul style="list-style-type: none"> "The major updated point on Ver.100_100 is that TIR phase correction. There are no change in SWIR processing so there is no difference in SWIR spectrum between current Ver.080_080 and Ver.100_100." - e-mail from Akihiro Matsushima |
| Version130130 | 110419–120418 | <ul style="list-style-type: none"> Preliminary Band-1 analog circuit non-linearity correction, based on ADC non-linearity implemented. Adjustment of saturation detection. Modification to TIR calibration. No v2.10 ACOS Level 2 data products produced with this version of GOSAT L1B |
| Version141141 | 090601–100731 | <ul style="list-style-type: none"> Modified correction to Band-1 analog circuit non-linearity Correction to the interferogram sampling interval uniformity Improvement of TIR phase correction |

| Version | Period YYMMDD | Changes |
|-------------------|--|---|
| Version006006 (P) | 090423–090504 090516–090728 | <ul style="list-style-type: none"> initial version |
| | | <ul style="list-style-type: none"> Improvement of the Band-1 scan speed instability correction for medium gain (Gain M) data. Processed using the 32-bit Level-1 processing system No v2.10 ACOS Level 2 data products produced with this version of GOSAT L1B |
| Version150150 | 120419-120619 | <ul style="list-style-type: none"> Identical to v141141, but processed on the 64-bit L1B production processing system |
| Version150151 | 090423 - 091031* 101224 - 111130* 120620-current | <ul style="list-style-type: none"> Identical to v150150, but with a corrected glint flag. *All L1B data will be reprocessed to this version by December 2012. |
| Version161160 | 090422 - 140607 | <ul style="list-style-type: none"> An optical path difference (OPD) sampling interval non-uniformity correction (SINUC) was applied in L1B V150. However, a spectral ringing artifact was inadvertently introduced to the spectra in the L1B V150 processing, as 100 zeros were filled in at both ends of the interferogram. The L1B V161 processing switched off SINUC to correct this mistake An update to how the calibration of the TANSO FTS thermal infrared measurement in spectral band 4 is performed. V161 includes a more accurate polarization reflectance for each mirror. |
| Version 201201 | 090422 - 160331 | <ul style="list-style-type: none"> Bug Fix of unexpected values of some data-sets (ZPD_MissFlag, masterQualityFlag, ZPD_ShiftFlag, satelliteAttitudeStabilityFlag and attributes of dataset) and the condition of ZPD Bias Correction. |
| Version 201202 | 160401 – Current | <ul style="list-style-type: none"> Latest version of GOSAT L1B |

The GOSAT team at JAXA produces GOSAT TANSO-FTS Level 1B (L1B) data products for internal use and for distribution to collaborative partners, such as ESA and NASA. These calibrated products are augmented by the ACOS Project with additional geolocation information and further corrections. These ACOS Level 1B products (with calibrated radiances and geolocation) are the input to the ACOS Level 2 production process.

The distribution of GOSAT and ACOS L1B products is currently restricted by cooperation agreements between JAXA and NASA.

3.4. ACOS Algorithms

In the sections that follow, the following definitions apply:

- Footprint – an observation by a single instrument
- Sounding – a combined observation of all instruments
- Granule – the construct expressing the content of a product (ACOS product granules contain all the processed GOSAT data for a single orbit)

3.4.1. Level 1B Algorithm Overview

The ACOS Level 1B (L1B) algorithm adds additional calibration information to the GOSAT TANSO-FTS Level 1B data, and converts these data to the format needed for the ACOS Level 2

algorithm. For example, the TANSO-FTS L1B is delivered with radiances expressed in engineering units (volts). JAXA provides a series of calibration tables that are used to convert these values from engineering units to the radiometric units used in the ACOS algorithm ($\text{photons/m}^2/\text{sr/cm}^{-1}$). The calibration information provided in these tables is derived from pre-launch calibration tests and on-orbit observations of internal light sources, deep space, the sun, the moon, and observations of calibration targets on the surface of the Earth. These tabulated results are assumed to be constant, or used to establish trends for time-dependent corrections.

Sounding and spacecraft geometric variables are included in the ACOS Level 2 products. Starting with v2.9, these geometric data are updated by the ACOS team, based on pointing error estimates provided by the GOSAT Project Team. As noted above, the pointing error tables applied to v2.9 are based on observations collected prior to December 2010, and are assumed to be constant in time. Some aspects of the geolocation is performed by the ACOS team based on standard Earth geoid shape and a high-resolution digital elevation model (DEM) and some is copied from the GOSAT input products.

ACOS does not currently process all soundings collected by GOSAT. Because the thermal IR data is not utilized in ACOS, only the soundings in the daylight portion of the GOSAT orbit are processed. This version of processing supports both nadir and glint soundings. Details of glint soundings are provided in section 2.5.2.

In addition, to restrict the attempted retrievals to those with adequate signal, the soundings are also screened by the expression “*sounding_solar_zenith* < 85”.

Performing retrievals on scenes containing clouds will either fail or have skewed results (depending upon the extent of cloud coverage). Users should check the *cloud_flag* for the ACOS estimate of scene cloudiness. Many cloudy scenes that are inadvertently passed by the cloud screen algorithm will not converge during the processing and, therefore, will not appear in the Level 2 retrieval results.

3.4.2. Level 2 Algorithm Overview

The Full-physics XCO₂ retrieval algorithm is based on the one that was to be used for the Orbiting Carbon Observatory (OCO). The algorithm is a Rodgers [2000]-type optimal estimation approach and has been described fully in O'Dell *et al.* [2011]. The retrieval algorithm consists of a forward model, an inverse method, and an error analysis step. The overall flow for the retrieval process is shown in Figure 5.

The basic idea is to use a forward model to simulate all three bands of the OCO-2 spectrum then fitting the measured spectra to the model. The forward model contains components simulating the solar spectrum, atmospheric scattering and absorption, surface optical properties, radiative transfer, and detection by the instrument. The input to the forward model consists of meteorological conditions, surface properties, characteristics of the instrument, etc. Everything that is necessary to fully simulate the as-measured radiances must be input to the forward model.

The residuals between the simulated and measured spectra are minimized by changing parameters in the state vector via the inverse method. This inversion is relatively efficient because the forward model returns not just simulated radiances, but also partial derivatives of those radiances, also called Jacobians. The Jacobians are used by the inverse model to efficiently update the state vector in order to quickly find the state that minimizes the residuals.

Once the atmospheric state yielding the best match to the observed spectrum has been found, the algorithm then determines X_{CO_2} , errors in X_{CO_2} from different sources (such as vertical smoothing, measurement noise, etc.), and the X_{CO_2} column averaging kernel. This is necessary because x_{CO_2} is not itself an element of the state vector. Rather, it is determined from the profile of CO_2 , which is part of the state vector. It is formally given by the total number of CO_2 molecules in the column divided by the total number of dry air molecules in the column. This step is labeled “Error Analysis” in Figure 5.

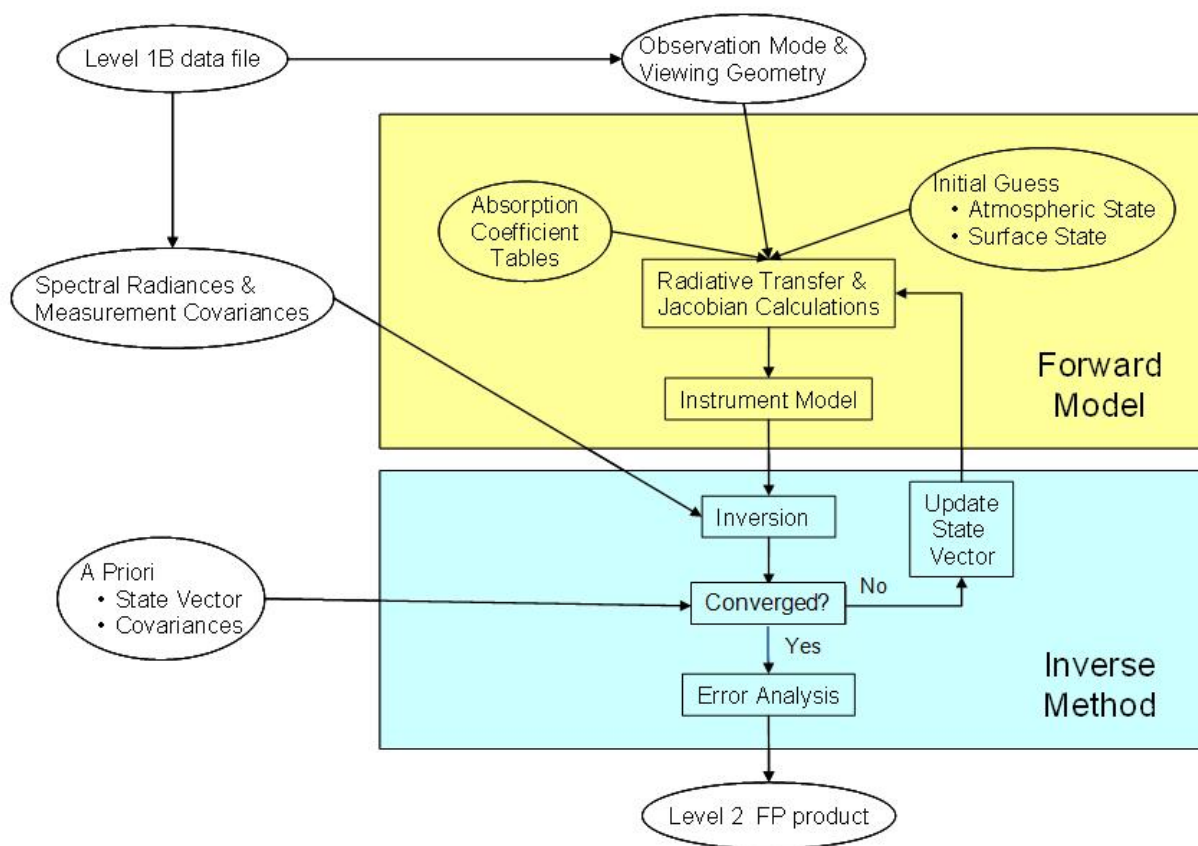


Figure 5: Level 2 Full Physics Retrieval Flow

3.5. ACOS Data Products

The ACOS Level 2 product set consists of products that focus on measuring column-averaged CO_2 dry air mole fraction (X_{CO_2}). The measurements are extracted from observations made by JAXA’s Greenhouse gases Observing SATellite (GOSAT). The global coverage that is achieved by GOSAT is repeated every three days at the highest resolution yet achieved from orbit.

3.5.1. File Naming Convention

ACOS Level 2 Product file name specification:

acos_ttt_date_nn_collection_productionTimeStamp.h5

Where:

- ttt = product type (L2s)
- date = observation date (yymmdd)
- nn = GOSAT path number (01-44)
- collection label, which consists of the following elements:
 - “Production”: indicates a production product
 - v[nnn][mmm]: the TANSO-FTS L1B product version where [nnn] is the algorithm version and [mmm] is the parameter version
 - [software component][version] = the software component and version number that created the product. The software component for the final product is always ‘L2s’. The version number for this release is ‘30504’.
 - r[nn] = the reprocessing level; initial production value is always ‘01’
 - Pol[x] = the polarization used for the retrievals; possible values are S, P, or B (both)
- productionTimeStamp = production date/time (UTC) at ACOS (yymmddhhmmss)

Filename examples:

acos_L2s_090724_07_Production_v110110_L2s2800_r01_PolB_101204185614.h5

acos_L2s_101102_43_Production_v100100_L2s20900_r01_PolB_111002175250.h5

By policy, *collection* will contain the software *build_id*. In addition, *collection* will also contain a data product version *rNN* in case the same product gets regenerated.

3.5.2. File Format and Structure

All ACOS Level 2 product files are in HDF-5 format, developed at the National Center for Supercomputing Applications <http://www.hdfgroup.org/>. This format facilitates the creation of logical data structures.

All ACOS Level 2 product files contain data structures indexed by sounding (1 to N soundings/file) and are associated by the *sounding_id* variable in all products.

Variables are combined into groups by type (e.g., SoundingGeometry). Within each type, a variable has one or more values per sounding. Variables may be single-valued (e.g., *sounding_altitude*) or multi-valued (e.g., *co2_profile*).

The metadata of each variable describes the variable's attributes, such as dimensions, data representation and units.

3.5.3. Data Definition

The ACOS Level 2 products contain many variables with a variety of dimensions. The following list describes only the most important of the dimensions.

- Retrieval the number of retrievals reported (those soundings for which retrievals converged or were converging when the maximum number of iterations was reached)
- Polarization the number of polarization states

- Level the number of atmospheric retrieval levels
- Exposure the number of scans in granule
- Band the number of spectral bands
- Aerosol the number of retrieval aerosol types

3.5.4. Global Attributes

In addition to variables and arrays of variables, global metadata is stored in the files. Some metadata are required by standard conventions, some are present to meet data provenance requirements and others as a convenience to users of the ACOS Level 2 Products. The most useful global attributes present in all files are shown in Table 4. Table 5 provides a list of key metadata fields for each variable.

Table 4: Some Global Metadata Attributes

| Global Attribute | Type | Description |
|---------------------------|----------------|---|
| AscendingNodeCrossingDate | String | The date of the ascending node crossing immediately before the first exposure in the TANSO-FTS file. Format: yyyy-mm-dd |
| AscendingNodeCrossingTime | String | The time of the ascending node crossing immediately before the first exposure in the TANSO-FTS file. Format: hh:mm:ss.sssZ |
| StartPathNumber | 32-bit integer | The first orbital path on which data contained in the product was collected. |
| StopPathNumber | 32-bit integer | The last orbital path on which data contained in the product was collected. |
| ProductionDateTime | String | The date and time at which the product was created. |
| CollectionLabel | String | Label associating files in a collection. |
| HDFVersionId | String | For example 'HDF5 1.8.5'. A character string that identifies the version of the HDF (Hierarchical Data Format) software that was used to generate this data file. |
| BuildId | String | The identifier of the build containing the software that created the product. |
| TFTSVersion | String | The version of the TANSO FTS data used to create this data product. |

Table 5: Key Metadata Items

| Name | Type | Description |
|---------|--------|--|
| Name | String | The name of the variable |
| Shape | String | The set of dimensions defining the structure |
| Type | String | The data representation type |
| Units | String | The units of the variable. |
| Minimum | String | Smallest valid value of the variable |
| Maximum | String | Largest valid value of the variable |

3.5.5. ACOS Metadata and Variables

This section contains tables describing the groups of variables and metadata elements for the ACOS product.

Table 6 provides information on ACOS metadata.

Table 6: Metadata Information

| Element | Storage | Comment |
|----------------------------------|---------|---|
| AbscoCO2Scale | Float32 | Empirical scaling factors for CO2 ABSCO tables. Values should be different for the 1.6 micron and 2.06 micron bands and were chosen to provide agreement of retrieved XCO2 with TCCON XCO2. |
| AbscoH2OScale | Float32 | Empirical scaling factor for H2O ABSCO tables. Currently should be 1.0. |
| AbscoO2Scale | Float32 | Empirical scaling factor for O2 ABSCO tables. Values chosen to improve agreement between retrieved surface pressure and independent estimates from a numerical weather prediction model. |
| AncillaryDataDescriptors | String | An array of file names that specifies all of the ancillary data files that were used to generate this output product. Ancillary data sets include all input except for the primary input files. |
| AscendingNodeCrossingDate | String | The date of the ascending node crossing immediately before the first exposure in the TANSO-FTS file. Format: yyyy-mm-dd |
| AscendingNodeCrossingTime | String | The time of the ascending node crossing immediately before the first exposure in the TANSO-FTS file. Format: hh:mm:ss.sssZ |
| AutomaticQualityFlag | String | Reserved for future use. |
| BuildId | String | The identifier of the build containing the software that created the product. |
| CollectionLabel | String | Label associating files in a collection |
| DataFormatType | String | 'NCSA HDF' - A character string that describes the internal format of the data product. |
| FirstSoundingId | | The <i>sounding_id</i> of the first sounding in the file |
| GranulePointer | String | The name of the product. |
| HDFVersionId | String | 'HDF5 vvvvvv' - A character string that identifies the version of the HDF (Hierarchical Data Format) software that was used to generate this data file where vvvvvv is a version id. |
| InputPointer | String | The name of the data product that provides the major input that was used to generate this product. |
| InstrumentShortName | String | 'TANSO-FTS' - The name of the instrument that collected the telemetry data. |
| L2FullPhysicsAlgorithmDescriptor | String | A short description of the Full-Physics algorithm that was used to generate this product |
| L2FullPhysicsDataVersion | String | Indicates the build version number of the Full-physics algorithm used. |
| L2FullPhysicsExeVersion | String | Indicates the build version number of the Full-physics algorithm used. |
| L2FullPhysicsInputPointer | String | List of the input files used by the Full-physics algorithm code |
| L2FullPhysicsProductionLocation | String | |
| LastSoundingId | Int64 | The <i>sounding_id</i> of the last sounding in the file |
| LongName | String | A complete descriptive name for the product. |

| Element | Storage | Comment |
|-------------------------|---------|--|
| MissingExposures | Int32 | Number of expected points missing from the dataset |
| NominalDay | String | The approximate date on which the data were acquired. A <i>NominalDay</i> starts at an orbit boundary, so the <i>NominalDay</i> for some data do not match their calendar day. Format: yymmdd |
| NumberOfExposures | Int32 | Actual number of points reported in the product |
| NumberOfGoodRetrievals | Int32 | Number of retrievals with master_quality_flag of Good |
| OrbitOfDay | Int8 | The ordinal number of the orbit within its <i>NominalDay</i> , starting with 1. |
| PlatformLongName | String | 'Greenhouse gases Observing SATellite' |
| PlatformShortName | String | 'GOSAT' |
| PlatformType | String | 'spacecraft' - The type of platform associated with the instrument which acquires the accompanying data |
| ProcessingLevel | String | Indicates processing level. The allowed values are: Level 1A, Level 1B, Level 2 |
| ProducerAgency | String | 'NASA' - Identification of the agency that provides the project funding |
| ProducerInstitution | String | 'JPL' - Identification of the institution that provides project management. |
| ProductionDateTime | String | The date and time at which the product was created. |
| ProductionLocation | String | Facility in which the file was produced: "Operations Pipeline", "Test Pipeline", "SCF", "Preflight Instrument Characterization", "Development", "Orbital", "Unknown" |
| ProductionLocationCode | String | One-letter code indicating the <i>ProductionLocation</i> . The allowed values are: "" (null string) - Operations Pipeline s - SCF t - Test Pipeline c - Preflight Instrument Characterization d - Development o - Orbital x - Unknown |
| ProjectId | String | 'ACOS' - The project identification string. |
| QAGranulePointer | String | A pointer to the quality assurance product that was generated with this product. |
| RangeBeginningDate | String | The date on which the earliest data contained in the product were acquired. Format: yyyy-mm-dd |
| RangeBeginningTime | String | The time at which the earliest data contained in the product were acquired. Format: hh:mm:ss.sssZ |
| RangeEndingDate | String | The date on which the latest data contained in the product were acquired. Format: yyyy-mm-dd |
| RangeEndingTime | String | The time at which the latest data contained in the product were acquired. |
| RetrievalIterationLimit | Int32 | Maximum number of iterations allowed in the implementation of the retrieval algorithm |

| Element | Storage | Comment |
|-----------------------|---------|--|
| RetrievalPolarization | String | Polarization used in TANSO-FTS measurements in this granule - "P", "S", or "B" (for Both). |
| ShortName | String | The short name used to identify all data granules in a given data collection. |
| SISName | String | The name of the document describing the contents of the product. |
| SISVersion | String | The version of the document describing the contents of the product. |
| SizeMBECSDataGranule | Float32 | The size of this data granule in Megabytes. |
| SpectralChannel | String | The identifier of the spectral regions present in this granule. Allowed values are: '0.76um O2 A-band', '1.6um Weak CO2', '2.06um Strong CO2' |
| StartPathNumber | Int32 | The first orbital path on which data contained in the product was collected. |
| StopPathNumber | Int32 | The last orbital path on which data contained in the product was collected. |
| TFTSVersion | String | The version of the TANSO FTS data used to create this data product. |
| VMRO2 | Float32 | The Volume Mixing Ratio of atmospheric O2 in units of Mole Mole ⁻¹ |

Table 7 describes variables related to the position of the spacecraft at the observation time. Note the variables have a Shape of 'Retrieval_Array'. Therefore, soundings are included only when retrievals converged or were converging when the maximum number of iterations was reached.

Table 7: Spacecraft Geometry Variables

| Element | Type | Unit | Min | Max | Comment |
|-------------------|---------|--------------------------------|------|-----|--|
| ground_track | Float32 | Degrees | 0 | 360 | Azimuth of the spacecraft ground track (measured from North) |
| relative_velocity | Float32 | Meters Second ⁻¹ | | | The component of the relative SC/Target motion along the look-vector. |
| spacecraft_alt | Float32 | Meters | | | Altitude of the spacecraft above the reference ellipsoid at the start of the exposure. |
| spacecraft_lat | Float32 | Degrees | -90 | 90 | Geodetic latitude of sub-spacecraft point at the start of the exposure. |
| spacecraft_lon | Float32 | Degrees | -180 | 180 | Longitude of sub-spacecraft point at the start of the exposure. |
| x_pos | Float32 | Meters | | | Spacecraft position in Earth Centered Rotating (ECR) coordinates at the start of the exposure. |
| x_vel | Float32 | Meters Second ⁻¹ | | | Spacecraft velocity in Earth Centered Rotating (ECR) coordinates at the start of the exposure. |
| y_pos | Float32 | Meters | | | Spacecraft position in Earth Centered Rotating (ECR) coordinates at the start of the exposure. |
| y_vel | Float32 | Meters Second ⁻¹ | | | Spacecraft velocity in Earth Centered Rotating (ECR) coordinates at the start of the exposure. |
| z_pos | Float32 | Meters | | | Spacecraft position in Earth Centered Rotating (ECR) coordinates at the start of the exposure. |
| z_vel | Float32 | Meters Second ⁻¹ | | | Spacecraft velocity in Earth Centered Rotating (ECR) coordinates at the start of the exposure. |

Table 8 describes variables related to the instrument look vector or the intersection of the look vector with the Earth surface. Note that the variables have a Shape of 'Retrieval_Array'. Therefore, soundings are included only when retrievals converged or were converging when the maximum number of iterations was reached.

Table 8: Sounding Geometry Variables

| Element | Type | Unit | Min | Max | Comment |
|----------------------------|---------|---------|------|-----|--|
| sounding_altitude | Float32 | Meters | | | Mean altitude of the surface within the sounding based on PGS Toolkit topography |
| sounding_altitude_max | Float32 | Meters | | | Maximum altitude of the surface within the sounding based on PGS Toolkit topography |
| sounding_altitude_min | Float32 | Meters | | | Minimum altitude of the surface within the sounding based on PGS Toolkit topography |
| sounding_altitude_stddev | Float32 | Meters | | | Standard deviation of the measure of altitude of the surface within the sounding |
| sounding_altitude_uncert | Float32 | Meters | | | Uncertainty of the measure of altitude of the surface within the sounding based on the accuracy of the input information |
| sounding_aspect | Float32 | Degrees | 0 | 360 | Azimuth of the surface projection of the slope surface normal |
| sounding_at_angle | Float32 | Degrees | -180 | 180 | Angle between the look vector and the spacecraft Y-Z plane. Positive angle is the right-hand screw direction of the Y-axis. |
| sounding_at_angle_error | Float32 | Degrees | -180 | 180 | The difference between AT value derived by MMO and actual one is stored |
| sounding_azimuth | Float32 | Degrees | 0 | 360 | Azimuth of the vector toward the instantaneous position of the spacecraft from the center of the sounding based on topography |
| sounding_ct_angle | Float32 | Degrees | -180 | 180 | Angle between look vector and the spacecraft X-Z plane. Positive angle direction is the right-hand screw direction of the X-axis |
| sounding_ct_angle_error | Float32 | Degrees | -180 | 180 | The difference between CT value derived by MMO and actual one is stored |
| sounding_glnt_angle | Float32 | Degrees | 0 | 180 | The angle between the vector to the glint spot and the actual look vector. |
| sounding_land_fraction | Float32 | Percent | 0 | 100 | Percent of land cover within the sounding. |
| sounding_latitude | Float32 | Degrees | -90 | 90 | Geodetic latitude of the center of the sounding based on PGS Toolkit topography |
| sounding_latitude_geoid | Float32 | Degrees | -90 | 90 | Geodetic latitude of the center of the sounding based on standard geoid |
| sounding_longitude | Float32 | Degrees | -180 | 180 | Longitude of the center of the sounding based on PGS Toolkit topography |
| sounding_longitude_geoid | Float32 | Degrees | -180 | 180 | Longitude of the center of the sounding based on standard geoid |
| sounding_plane_fit_quality | Float32 | Meters | | | Standard deviation for the tangent plane approximation |
| sounding_slope | Float32 | Degrees | 0 | 90 | Slope of the best-fit plane to the surface within the sounding. |
| sounding_solar_azimuth | Float32 | Degrees | 0 | 360 | Azimuth of the sun at the center of the sounding based on topography |

| Element | Type | Unit | Min | Max | Comment |
|-----------------------|---------|---------|-----|-----|--|
| sounding_solar_zenith | Float32 | Degrees | 0 | 90 | Angle between the normal to the Earth geoid and the solar angle at the center of the sounding based on topography |
| sounding_zenith | Float32 | Degrees | 0 | 90 | The angle between the normal to the Earth geoid and the vector toward the instantaneous position of the spacecraft from the center of the sounding based on topography |

Table 9 describes Sounding Header fields. They all have the Shape 'Exposure_Array' and, therefore, include all soundings.

Table 9: Sounding Header Variables

| Element | Type | Comment |
|------------------------|-----------|--|
| cloud_flag | Int8 | Estimate of scene visibility for this <i>sounding_id</i> taken from an ABO2-only clear sky retrieval: 0 - Clear, 1 - Cloudy, 2 - Undetermined |
| l2_packaging_qual_flag | BitField8 | Bit Flags are used to record the status of each sounding during packaging of l2 output into retrieval arrays. See Table 16. |
| retrieval_index | Int32 | Index into the Retrieval dimension of arrays in the RetrievalResults group for soundings associated with retrievals. |
| sounding_id | Int64 | The unique identifier of the sounding. |

Table 10 describes data products related to cloud screening.

To further reduce the computation time of retrievals containing clouds, a cloud screening algorithm is applied to this version. It performs a fast, Oxygen A-band only clear-sky retrieval for surface pressure, surface albedo, temperature offset and dispersion multiplier. The retrieved surface pressure and albedo information are combined with the χ^2 goodness-of-fit statistic and signal-to-noise ratio to determine if a scene is clear (0), cloudy (1), or undetermined (2) as shown in Table 10. See Section 6 for a paper on this topic.

Table 10: A-Band-only Retrieval Variables

| Element | Type | Comment |
|--------------------------------------|---------|---|
| albedo_o2_cld | Float32 | Retrieved value of lambertian surface albedo at 785 and 755 nm, respectively; from the O2 A Band cloud retrieval. |
| dispersion_multiplier_cld | Float64 | The retrieved wavenumber multiplier to get the best fit to the O2 A band; from the A Band cloud retrieval. |
| noise_o2_cld | Float32 | The noise level in the O2 A band for (P+S)/2, averaged over the spectral samples with the ten highest radiance levels. |
| reduced_chi_squared_o2_cld | Float32 | The reduced χ^2 value of the O2 A-band clear-sky fit used in determine the presence or absence of cloud; from the O2 A Band cloud retrieval. |
| reduced_chi_squared_o2_threshold_cld | Float32 | The threshold of reduced_chisquared_o2_cld above which cloud_flag is set to 1. |
| signal_o2_cld | Float32 | The signal level in the O2 A band for (P+S)/2, averaged over the spectral samples with the ten highest radiance levels. |

| Element | Type | Comment |
|------------------------------|---------|---|
| snr_o2_cld | Float32 | The value of the signal-to-noise ratio of (P+S)/2, averaged over the spectral samples with the ten highest radiance levels. |
| surface_pressure_apriori_cld | Float32 | The value of the surface pressure of the center of GOSAT's field-of-view estimated from ECMWF; from the O2 A Band cloud retrieval. |
| surface_pressure_cld | Float32 | The retrieved value of the surface pressure; from the O2 A Band cloud retrieval. |
| surface_pressure_delta_cld | Float32 | surface_pressure_cld - surface_pressure_apriori_cld - surface_pressure_offset_cld |
| surface_pressure_offset_cld | Float32 | The assumed surface pressure offset for clear-sky soundings, caculated from an empirical relation based on solar zenith angle, land/water and H/M gain; from the O2 A Band cloud retrieval. |
| temperature_offset_cld | Float32 | The retrieved offset to the assumed profile of temperature taken from the prior (ECMWF) meteorology; from the O2 A Band cloud retrieval. |

The IMAP-DOAS fields are listed in Table 11.

Table 11: IMAP-DOAS Retrieval Variables

| Element | Type | Comment |
|-------------------------------------|---------|---|
| ch4_column_apriori_idp | Float32 | A priori vertical column density of CH4 (climatology) |
| ch4_column_idp | Float32 | Vertical column density of CH4 (weak band) |
| ch4_column_uncert_idp | Float32 | 1-sigma error in the vertical column density of CH4 |
| ch4_weak_band_processing_flag_idp | Int8 | 0=processed, 1=failed, 2=not processed |
| cloud_flag_idp | Int8 | Cloud&Aerosol filter flag; -2=unusable (outside of SZA range); -1=not all retrievals converged; 0=clearly cloudy; 1=probably cloudy; 2=probably clear; 3=very clear |
| co2_column_apriori_idp | Float32 | A priori vertical column density of CO2 (climatology) |
| co2_column_ch4_window_idp | Float32 | Vertical column density of CO2 retrieved in the CH4 fit window (very weak lines) |
| co2_column_strong_band_idp | Float32 | Vertical column density of CO2 (strong band) |
| co2_column_strong_band_uncert_idp | Float32 | 1-sigma error in the vertical column density of CO2 (strong band) |
| co2_column_weak_band_idp | Float32 | Vertical column density of CO2 (weak band) |
| co2_column_weak_band_uncert_idp | Float32 | 1-sigma error in the vertical column density of CO2 |
| co2_ratio_idp | Float32 | Ratio of retrieved CO2 column (no scattering code) in weak and strong CO2 ban |
| co2_strong_band_processing_flag_idp | Int8 | 0=processed, 1=failed, 2=not processed |
| co2_weak_band_processing_flag_idp | Int8 | 0=processed, 1=failed, 2=not processed |
| delta_d_idp | Float32 | Deuterium depletion of total column water vapor |
| delta_d_uncert_idp | Float32 | 1-sigma uncertainty in deuterium depletion of total column water vapor |
| dry_air_column_apriori_idp | Float32 | Integrated vertical column of dry airmass derived from meteorological data |
| h2o_column_apriori_idp | Float32 | A priori vertical column density of H2O (based on ECMWF) |
| h2o_column_idp | Float32 | Vertical column density of H2O |
| h2o_column_uncert_idp | Float32 | 1-sigma error in the vertical column density of H2O |
| h2o_ratio_idp | Float32 | Ratio of retrieved H2O column (no scattering code) in weak and strong CO2 band |
| h2o_ratio_uncert_idp | Float32 | 1-sigma uncertainty in the ratio of retrieved H2O column (no scattering code) in weak and strong CO2 band |
| hdo_column_apriori_idp | Float32 | A priori vertical column density of HDO |
| hdo_column_idp | Float32 | Vertical column density of HDO |
| hdo_column_uncert_idp | Float32 | 1-sigma error in the vertical column density of HDO |
| hdo_h2o_processing_flag_idp | Int8 | 0=processed, 1=failed, 2=not processed |

| | | |
|---------------------------------------|---------|--|
| o2_ratio_p_idp | Float32 | Ratio of retrieved and ECMWF O2 column retrieved in P-polarization |
| o2_ratio_s_idp | Float32 | Ratio of retrieved and ECMWF O2 column retrieved in S-polarization |
| out_of_band_transmission_p_idp | Float32 | Transmission at the band-pass edge, P-polarization, band 1 |
| out_of_band_transmission_s_idp | Float32 | Transmission at the band-pass edge, S-polarization, band 1 |
| total_offset_fit_relative_755nm_p_idp | Float32 | Total offset fit (0-level + fluorescence) as fraction of continuum level (755nm, P polarization) |
| total_offset_fit_relative_755nm_s_idp | Float32 | Total offset fit (0-level + fluorescence) as fraction of continuum level (755nm, S polarization) |
| total_offset_fit_relative_771nm_p_idp | Float32 | Total offset fit (0-level + fluorescence) as fraction of continuum level (771nm, P polarization) |
| total_offset_fit_relative_771nm_s_idp | Float32 | Total offset fit (0-level + fluorescence) as fraction of continuum level (771nm, S polarization) |

Table 12 describes the Retrieval Header, providing general characteristics of the soundings retrieved. Soundings are included only when retrievals converged or were converging when the maximum number of iterations was reached.

Table 12: Retrieval Header Variables

| Element | Type | Comment |
|-----------------------|-----------|--|
| acquisition_mode | String | The instrument mode in which the data in the product were collected. Valid values are: 'OB1D', 'OB1N', 'OB2D', 'SPOD', 'SPON', 'CALM', 'LUCA' |
| ct_observation_points | Int8 | Number of observation points in the cross track direction -1: undefined or specified observation, 0: Electrical Calibration, "0x01" : 1 points "0x03" : 3 points "0x05" : 5 points "0x07" : 7 points "0x09" : 9 points |
| exposure_duration | Float32 | The duration of the exposure |
| exposure_index | Int32 | The index into the Exposure dimension of arrays in SoundingHeader, SoundingGeometry, and SpacecraftGeometry groups containing the spectra used to perform the retrieval |
| gain_swir | String | Instrument gain setting for each polarization: H - High gain, M - Medium gain, L - Low gain, H_ERR - Error in setting high gain, M_ERR - Error in setting medium gain, L_ERR - Error in setting low gain, UNDEF - Gain set to an undefined state |
| glint_flag | Int8 | This field is incorrect after YYYY-MM-DD. Use the glint filter described in section XXX instead of the glint_flag. Indicates whether GOSAT was in glint mode when acquiring the sounding 0 = Not in glint mode 1 = In glint mode |
| sounding_id_reference | Int64 | The sounding_id of the sounding containing the spectra used to perform the retrieval |
| sounding_qual_flag | BitFlag32 | Single-bit quality flags. See Table 16. |
| sounding_time_string | String | Representative sounding time, in the format yyyy-mm-ddThh:mm:ss.sssZ |
| sounding_time_tai93 | Float64 | Sounding time in number of SI seconds since midnight, January 1, 1993. |
| spike_noise_flag | Int8 | 0 - No spike noise present, 1 - Spike noise present |

| Element | Type | Comment |
|---------------------|------|--|
| warn_level | Int8 | Provides a value that summarizes each sounding's acceptability to a larger set of quality filters. A high warn_level predicts that the sounding would fail most data filters applied to it. A low warn_level suggests that the sounding would pass most quality filters that might be applied. Min=0, Max=19 |
| zpd_saturation_flag | Int8 | Copy exposureAttribute/pointAttribute/RadiometricCorrectionInfo/ZPD_SatiratomFlag_SWIR |

Table 13 describes variables expressing the retrieval results. Note that some of the variables have a Shape including 'Retrieval'. Therefore, soundings are included only when retrievals converged or were converging when the maximum number of iterations was reached.

In Table 13, $xco2$ is calculated in the following way:

$$xco2 = \sum_{i=1}^{N_{num_levels}} W_i CO2_i$$

where W_i represents $xco2_pressure_weighting_function$ and $CO2_i$ represents $co2_profile$. The sum is over num_levels . W_i is a function primarily of the pressure level spacing, but also weakly of water vapor, and also depends on surface pressure.

Table 13: Variables Expressing Retrieval Results

| Element | Type | Comment |
|--------------------------------------|---------|---|
| aerosol_1_aod | Float32 | Retrieved total column-integrated aerosol optical depth for aerosol type 1 |
| aerosol_1_aod_high | Float32 | Retrieved column-integrated aerosol optical depth of aerosol type 1 for pressure levels less than 50,000 Pa |
| aerosol_1_aod_low | Float32 | Retrieved column-integrated aerosol optical depth of aerosol type 1 for pressure levels greater than 80000 Pa |
| aerosol_1_aod_mid | Float32 | Retrieved column-integrated aerosol optical depth of aerosol type 1 for pressure levels between 50,000 and 80,000 Pa |
| aerosol_1_gaussian_log_param | Float32 | Retrieved gaussian log parameters for aerosol type 1 [total log aod, center pressure/surf-pressure, pressure sigma/surf-pressure] |
| aerosol_1_gaussian_log_param_apriori | Float32 | a priori of retrieved gaussian log parameters for aerosol type 1 |
| aerosol_1_gaussian_log_param_uncert | Float32 | Uncertainty of retrieved gaussian log parameters for aerosol type 1 |

| Element | Type | Comment |
|--------------------------------------|---------|---|
| aerosol_2_aod | Float32 | Retrieved total column-integrated aerosol optical depth for aerosol type 2 |
| aerosol_2_aod_high | Float32 | Retrieved column-integrated aerosol optical depth of aerosol type 2 for pressure levels less than 50,000 Pa |
| aerosol_2_aod_low | Float32 | Retrieved column-integrated aerosol optical depth of aerosol type 2 for pressure levels greater than 80,000 Pa |
| aerosol_2_aod_mid | Float32 | Retrieved column-integrated aerosol optical depth of aerosol type 2 for pressure levels between 50,000 and 80,000 Pa |
| aerosol_2_gaussian_log_param | Float32 | Retrieved gaussian log parameters of aerosol type 2 [total log aod, center pressure/surf-pressure, pressure sigma/surf-pressure] |
| aerosol_2_gaussian_log_param_apriori | Float32 | a priori of retrieved gaussian log parameters for aerosol type 2 |
| aerosol_2_gaussian_log_param_uncert | Float32 | Uncertainty of retrieved gaussian log parameters for aerosol type 2 |
| aerosol_3_aod | Float32 | Retrieved total column-integrated aerosol optical depth for aerosol type 3 |
| aerosol_3_aod_high | Float32 | Retrieved column-integrated aerosol optical depth of aerosol type 3 for pressure levels less than 50,000 Pa |
| aerosol_3_aod_low | Float32 | Retrieved column-integrated aerosol optical depth of aerosol type 3 for pressure levels greater than 80,000 Pa |
| aerosol_3_aod_mid | Float32 | Retrieved column-integrated aerosol optical depth of aerosol type 3 for pressure levels between 50,000 and 80,000 Pa |
| aerosol_3_gaussian_log_param | Float32 | Retrieved gaussian log parameters for aerosol type 3 [total log aod, center pressure/surf-pressure, pressure sigma/surf-pressure] |
| aerosol_3_gaussian_log_param_apriori | Float32 | a priori of retrieved gaussian log parameters for aerosol type 3 |
| aerosol_3_gaussian_log_param_uncert | Float32 | Uncertainty of retrieved gaussian log parameters of aerosol type 3 |
| aerosol_4_aod | Float32 | Retrieved total column-integrated aerosol optical depth for aerosol type 4 |
| aerosol_4_aod_high | Float32 | Retrieved column-integrated aerosol optical depth of aerosol type 4 for pressure levels less than 50,000 Pa |
| aerosol_4_aod_low | Float32 | Retrieved column-integrated aerosol optical depth of aerosol type 4 for pressure levels greater than 80,000 Pa |
| aerosol_4_aod_mid | Float32 | Retrieved column-integrated aerosol optical depth of aerosol type 4 for pressure levels between 50,000 and 80,000 Pa |

| Element | Type | Comment |
|--------------------------------------|---------|---|
| aerosol_4_gaussian_log_param | Float32 | Retrieved gaussian log parameters for aerosol type 4 [total log aod, center pressure/surf-pressure, pressure sigma/surf-pressure] |
| aerosol_4_gaussian_log_param_apriori | Float32 | a priori of retrieved gaussian log parameters for aerosol type 4 |
| aerosol_4_gaussian_log_param_uncert | Float32 | Uncertainty of retrieved gaussian log parameters for aerosol type 4 |
| aerosol_total_aod | Float32 | Retrieved total column-integrated aerosol optical depth for all aerosol types |
| aerosol_total_aod_high | Float32 | Retrieved column-integrated aerosol optical depth for all aerosol types for pressure levels less than 50,000 Pa |
| aerosol_total_aod_low | Float32 | Retrieved column-integrated aerosol optical depth for all aerosol types for pressure levels greater than 80,000 Pa |
| aerosol_total_aod_mid | Float32 | Retrieved column-integrated aerosol optical depth for all aerosol types for pressure levels between 50,000 and 80,000 Pa |
| aerosol_types | String | Retrieved aerosol types Allowed values: DU, SS, BC, OC, SO, ice, water |
| albedo_apriori_o2_fph | Float32 | Apriori of retrieved Lambertian component of albedo at 0.77 microns |
| albedo_apriori_strong_co2_fph | Float32 | Apriori of retrieved Lambertian componet of albedo at 2.06 microns |
| albedo_apriori_weak_co2_fph | Float32 | Apriori of retrieved Lambertian component of albedo at 1.615 microns |
| albedo_o2_fph | Float32 | Retrieved Lambertian component of albedo at at 0.77 microns |
| albedo_slope_apriori_o2 | Float32 | Apriori of retrieved spectral dependence of Lamberion component of albedo within o2 channel |
| albedo_slope_apriori_strong_co2 | Float32 | Apriori of spectral dependence of Lamberion component of albedo within strong co2 channel |
| albedo_slope_apriori_weak_co2 | Float32 | Apriori of retrieved spectral dependence of Lamberion component of albedo within weak co2 channel |
| albedo_slope_o2 | Float32 | Retrieved spectral dependence of Lamberion component of albedo within o2 channel |
| albedo_slope_strong_co2 | Float32 | Retrieved spectral dependence of Lamberion component of albedo within strong co2 channel |
| albedo_slope_uncert_o2 | Float32 | Uncertainty of retrieved spectral dependence of Lamberion component of albedo within o2 channel |
| albedo_slope_uncert_strong_co2 | Float32 | Uncertainty of spectral dependence of Lamberion component of albedo within strong co2 channel |
| albedo_slope_uncert_weak_co2 | Float32 | Uncertainty of retrieved spectral dependence of Lamberion component of albedo within weak co2 channel |
| albedo_slope_weak_co2 | Float32 | Retrieved spectral dependence of Lamberion component of albedo within weak co2 channel |
| albedo_strong_co2_fph | Float32 | Retrieved Lambertian component of albedo at 2.06 microns |

| Element | Type | Comment |
|--------------------------------------|---------|--|
| albedo_uncert_o2_fph | Float32 | Uncertainty of retrieved Lambertian component of albedo at 0.77 microns |
| albedo_uncert_strong_co2_fph | Float32 | Uncertainty of retrieved Lambertian component of albedo at 2.06 microns |
| albedo_uncert_weak_co2_fph | Float32 | Uncertainty of retrieved Lambertian component of albedo at 1.615 microns |
| albedo_weak_co2_fph | Float32 | Retrieved Lambertian component of albedo at 1.615 microns |
| apriori_o2_column | Float32 | Apriori vertical column of O2 |
| co2_profile | Float32 | Vertical profile of CO ₂ |
| co2_profile_apriori | Float32 | Vertical apriori profile of CO ₂ |
| co2_profile_averaging_kernel_matrix | Float32 | Averaging kernel for co2 profile |
| co2_profile_covariance_matrix | Float32 | Covariance matrix for co2 profile |
| co2_profile_uncert | Float32 | Vertical profile of CO ₂ uncertainty |
| dispersion_offset_apriori_o2 | Float64 | Apriori of retrieved spectral shift in o2 channel |
| dispersion_offset_apriori_strong_co2 | Float64 | Apriori of retrieved dispersion offset term in strong co2 channel |
| dispersion_offset_apriori_weak_co2 | Float64 | Apriori of retrieved dispersion offset term in weak co2 channel |
| dispersion_offset_o2 | Float64 | Retrieved dispersion offset term in o2 channel |
| dispersion_offset_strong_co2 | Float64 | Retrieved dispersion offset term in strong co2 channel |
| dispersion_offset_uncert_o2 | Float32 | Uncertainty of retrieved dispersion offset term in o2 channel |
| dispersion_offset_uncert_strong_co2 | Float32 | Uncertainty of retrieved dispersion offset term in strong co2 channel |
| dispersion_offset_uncert_weak_co2 | Float32 | Uncertainty of retrieved dispersion offset term in weak co2 channel |
| dispersion_offset_weak_co2 | Float64 | Retrieved dispersion offset term in weak co2 channel |
| diverging_steps | Int16 | Number of iterations in which solution diverged |
| dof_co2_profile | Float32 | Degrees of freedom (target gas profile only) |
| dof_full_vector | Float32 | Degrees of freedom (Full state vector) |
| eof_1_scale_apriori_o2 | Float32 | Apriori of retrieved scale factor of first empirical orthogonal residual function in o2 channel |
| eof_1_scale_apriori_strong_co2 | Float32 | Apriori of retrieved scale factor of first empirical orthogonal residual function in strong co2 channel |
| eof_1_scale_apriori_weak_co2 | Float32 | Apriori of retrieved scale factor of first empirical orthogonal residual function in weak co2 channel |
| eof_1_scale_o2 | Float32 | Retrieved scale factor of first empirical orthogonal residual function in o2 channel |
| eof_1_scale_strong_co2 | Float32 | Retrieved scale factor of first empirical orthogonal residual function in strong co2 channel |
| eof_1_scale_uncert_o2 | Float32 | Uncertainty of retrieved scale factor of first empirical orthogonal residual function in o2 channel |
| eof_1_scale_uncert_strong_co2 | Float32 | Uncertainty of retrieved scale factor of first empirical orthogonal residual function in strong o2 channel |
| eof_1_scale_uncert_weak_co2 | Float32 | Uncertainty of retrieved scale factor of first empirical orthogonal residual function in weak o2 channel |

| Element | Type | Comment |
|--|---------|---|
| eof_1_scale_weak_co2 | Float32 | Retrieved scale factor of first empirical orthogonal residual function in weak co2 channel |
| fluorescence_at_reference | Float32 | Retrieved fluorescence at 0.755 microns |
| fluorescence_at_reference_apriori | Float32 | Apriori of retrieved fluorescence at 0.755 microns |
| fluorescence_at_reference_uncert | Float32 | Uncertainty of retrieved fluorescence at 0.755 microns |
| fluorescence_slope | Float32 | Retrieved fluorescence slope at 0.755 microns |
| fluorescence_slope_apriori | Float32 | Apriori of retrieved fluorescence slope at 0.755 microns |
| fluorescence_slope_uncert | Float32 | Uncertainty of retrieved fluorescence slope at 0.755 microns |
| h2o_scale_factor | Float32 | Retrieved scale factor for h2o profile |
| h2o_scale_factor_apriori | Float32 | Apriori of retrieved scale factor for h2o profile |
| h2o_scale_factor_uncert | Float32 | Uncertainty of retrieved scale factor for h2o profile |
| iterations | Int16 | Number of iterations |
| last_step_levenberg_marquardt_parameter | Float32 | Levenberg Marquardt parameter corresponding to last iteration |
| num_active_levels | Int16 | Number of levels in atmospheric model |
| outcome_flag | Int8 | -2 = bad fill, -1 = packaging failure, 1 = passed internal quality check, 2 = failed internal quality check, 3 = reach max allowed iterations, 4 = reached max allowed divergences |
| retrieved_co2_column | Float32 | Retrieved vertical column of CO2 |
| retrieved_dry_air_column_layer_thickness | Float32 | Retrieved vertical column of dry air per atmospheric layer |
| retrieved_h2o_column | Float32 | Retrieved vertical column of H2O |
| retrieved_h2o_column_layer_thickness | Float32 | Retrieved vertical column of H2O per atmospheric layer |
| retrieved_o2_column | Float32 | Retrieved vertical column of O2 |
| retrieved_wet_air_column_layer_thickness | Float32 | Retrieved vertical column of wet air per atmospheric layer |
| specific_humidity_profile_ecmwf | Float32 | ECMWF specific humidity profile interpolated to observation location, time |
| surface_pressure_apriori_fph | Float32 | Apriori of surface pressure |
| surface_pressure_fph | Float32 | Surface pressure |
| surface_pressure_uncert_fph | Float32 | Apriori of surface pressure |
| surface_type | String | "Lambertian" or "Coxmunk,Lambertian" This element can be used to determine whether a sounding is in glint mode (Coxmunk,Lambertian) or nadir (Lambertian). |
| temperature_offset_apriori_fph | Float32 | Apriori of retrieved offset of temperature profile |
| temperature_offset_fph | Float32 | Retrieved offset of temperature profile |
| temperature_offset_uncert_fph | Float32 | Uncertainty of retrieved offset of temperature profile |

| Element | Type | Comment |
|----------------------------------|---------|--|
| temperature_profile_ecmwf | Float32 | ECMWF temperature profile interpolated to observation location, time |
| vector_pressure_levels | Float32 | Pressure altitude corresponding to each atmospheric level |
| vector_pressure_levels_apriori | Float32 | |
| vector_pressure_levels_ecmwf | Float32 | Pressure altitude corresponding to each ECMWF atmospheric level |
| wind_speed | Float32 | Retrieved Cox-Munk wind speed |
| wind_speed_apriori | Float32 | Apriori of retrieved Cox-Munk wind speed |
| wind_speed_uncert | Float32 | Uncertainty of retrieved Cox-Munk wind speed |
| xco2 | Float32 | Column-averaged CO2 dry air mole fraction |
| xco2_apriori | Float32 | Apriori of column-averaged CO2 dry air mole fraction. |
| xco2_avg_kernel | Float32 | Column averaging kernel |
| xco2_avg_kernel_norm | Float32 | Normalized column averaging kernel |
| xco2_pressure_weighting_function | Float32 | Pressure weighting function to form xco2 |
| xco2_uncert | Float32 | Error in column averaged target gas dry air mole fraction |
| xco2_uncert_interf | Float32 | Variance of target gas due to interference |
| xco2_uncert_noise | Float32 | Variance of target gas due to noise |
| xco2_uncert_smooth | Float32 | Variance of target gas due to smoothing |
| zero_level_offset_apriori_o2 | Float32 | Apriori of retrieved zero level offset in o2 channel |
| zero_level_offset_o2 | Float32 | Retrieved zero level offset in o2 channel |
| zero_level_offset_uncert_o2 | Float32 | Uncertainty of retrieved zero level offset in o2 channel |

Table 14 describes variables related to the analysis of the three spectral regions. Note that the variables have a Shape including 'Retrieval'. Therefore, soundings are included only when retrievals converged or were converging when the maximum number of iterations was reached.

In the descriptions below, "Reduced chi squared" is defined as:

$$\chi_r^2 = \frac{1}{N_{chan} - 5} \sum_{i=1}^{N_{chan}} \frac{(y_i - f_i(\hat{x}))^2}{\sigma_i^2}$$

where N_{chan} is the number of GOSAT channels in the spectral region, y_i is the radiance value measured by GOSAT in channel i , σ_i^2 is the square of the uncertainty (or noise) in channel i , and $f_i(x)$ is the model of the radiance in channel i .

Table 14: Spectral Parameter Variables

| Element | Type | Unit | Comment |
|--|---------|---------------------------------------|--|
| noise_o2_fph | Float32 | $W\ cm^{-2}\ sr^{-1}\ (cm^{-1})^{-1}$ | |
| noise_strong_co2_fph | Float32 | $W\ cm^{-2}\ sr^{-1}\ (cm^{-1})^{-1}$ | |
| noise_weak_co2_fph | Float32 | $W\ cm^{-2}\ sr^{-1}\ (cm^{-1})^{-1}$ | |
| reduced_chi_squared_o2_fph | Float32 | | Reduced chi squared of spectral fit for ABO2 spectral region |
| reduced_chi_squared_strong_co2_fph | Float32 | | Reduced chi squared of spectral fit for Strong CO2 spectral region |
| reduced_chi_squared_weak_co2_fph | Float32 | | Reduced chi squared of spectral fit for Weak CO2 spectral region |
| relative_residual_mean_square_o2 | Float32 | | Root mean squares of residuals over signal, i.e. $\sqrt{[1/N * \sum((MeasuredRadiance - ModelRadiance)/signal)^2]}$ where N is the number of spectral elements in the band |
| relative_residual_mean_square_strong_co2 | Float32 | | Root mean squares of residuals over signal, i.e. $\sqrt{[1/N * \sum((MeasuredRadiance - ModelRadiance)/signal)^2]}$ where N is the number of spectral elements in the band |
| relative_residual_mean_square_weak_co2 | Float32 | | Root mean squares of residuals over signal, i.e. $\sqrt{[1/N * \sum((MeasuredRadiance - ModelRadiance)/signal)^2]}$ where N is the number of spectral elements in the band |
| residual_mean_square_o2 | Float32 | $W\ cm^{-2}\ sr^{-1}\ (cm^{-1})^{-1}$ | Root mean squares of residuals |
| residual_mean_square_strong_co2 | Float32 | $W\ cm^{-2}\ sr^{-1}\ (cm^{-1})^{-1}$ | Root mean squares of residuals |
| residual_mean_square_weak_co2 | Float32 | $W\ cm^{-2}\ sr^{-1}\ (cm^{-1})^{-1}$ | Root mean squares of residuals |
| signal_o2_fph | Float32 | $W\ cm^{-2}\ sr^{-1}\ (cm^{-1})^{-1}$ | the signal level representative of the continuum level for this spectrum. |
| signal_strong_co2_fph | Float32 | $W\ cm^{-2}\ sr^{-1}\ (cm^{-1})^{-1}$ | The signal level representative of the continuum level for this spectrum. |
| signal_weak_co2_fph | Float32 | $W\ cm^{-2}\ sr^{-1}\ (cm^{-1})^{-1}$ | the signal level representative of the continuum level for this spectrum. |
| snr_o2_l1b | Float32 | | Signal-to-noise ratio for ABO2 spectral region . from the L1b processing |
| snr_strong_co2_l1b | Float32 | | Signal-to-noise ratio for Strong CO2 spectral region |
| snr_weak_co2_l1b | Float32 | | Signal-to-noise ratio for Weak CO2 spectral region |

Table 15 describes bit definitions for the three variables that are constructed as bit flags.

Table 15: Bit Flag Definitions

| Element | Bit # | Content |
|------------------------|-------|---|
| l2_packaging_qual_flag | 0 | Spare |
| | 1 | Spare |
| | 2 | excluded during sounding selection |
| | 3 | skipped due to missing sounding file |
| | 4 | skipped due to failed sounding file pre-check |
| | 5 | failed due to sounding file read error |
| | 6 | Spare |
| | 7 | failed due to unexpected packaging error |

| Element | Bit # | Content |
|--------------------|-------|---|
| sounding_qual_flag | 0 | Radiance calibration 0 = At least one band succeeded at least partially 1 = All three bands failed |
| | 1 | Geolocation 0 = Sounding geolocation succeeded 1 = Sounding geolocation failed |
| | 2 | Radiance calibration 0 = All three bands succeeded 1 = At least one band failed in at least one color |
| | 3 | Sounding geometry 0 = All parameters derived successfully 1 = Derivation failed |
| | 4 | Band ABO2 radiance calibration 0 = Successful 1 = At least on one color failed |
| | 5 | Band WCO2 radiance calibration 0 = Successful 1 = At least on one color failed |
| | 6 | Band SCO2 radiance calibration 0 = Successful 1 = At least on one color failed |
| | 7 | Sounding time derivation 0 = Successful 1 = Failed |
| | 8 | Derivation of surface parameters using DEM 0 = Successful 1 = Some parameters could not be derived |
| | 9 | Spacecraft position and velocity derivation 0 = Successful 1 = Failed |
| | 10-31 | Spare |

4. ACOS Level 2 Lite Data Products

With this delivery of the ACOS v7.3 data products, we have released a version of the OCO-2 Lite data files. The main differences between the Lite data file are that the files are aggregated on a daily basis, the files contain a streamlined set of output parameters (a subset of the full L2 data products) and they contain warn levels for the retrievals. The warn levels permit users to select the percentage of data to retain, with the “most trusted” soundings offered first. A description of the warn levels is provided in Mandrake et al., 2013. This OCO-2 document provides background information on warn levels and provides details on how warn levels were implemented for OCO-2. They were implemented for the ACOS data in a manner consistent with OCO-2. The primary difference between the OCO-2 implementation and the ACOS implementation of warn levels involves the range of possible values. The ACOS warn levels range from 0 (best quality) to 9 (lowest quality), in OCO-2 v7 data the range runs from 0 to 19. The change to the smaller range will be implemented in the next version of OCO-2 data as well.

Tables 16-19 provide a description of the variables available in the Lite data files. They are designed to be somewhat easier to use (smaller files, aggregated daily). The data included in these files are consistent with the Level 2 data products.

Table 16 provides a description of the fields in the ACOS Lite Data Product files.

| Element | Type | Unit | Comment |
|---------------------|---------|---------|--|
| co2_profile_apriori | Float32 | ppm | Prior CO2 Prior assumed by L2 code; Defined on layer boundaries. These are oriented space-to-surface, so the first element defines the TOA, the last element defines the surface. |
| date | Float32 | | Observation date and time matching sounding_id. |
| File_index | Float32 | | 1-Based Index of L2 File for each sounding |
| latitude | Float32 | Degrees | Center latitude of the measurement |
| longitude | Float32 | Degrees | Center longitude of the measurement"; |
| levels | Long | | Level counter |
| pressure_levels | Float32 | hPa | Pressure at each level; Defined on layer boundaries. These are oriented space-to-surface, so the first element defines the TOA, the last element defines the surface |
| pressure_weight | Float32 | | Pressure weighting function for each level; Defined on layer boundaries. These are oriented space-to-surface, so the first element defines the TOA, the last element defines the surface |
| sensor_zenith_angle | Float32 | Degrees | Zenith angle of the satellite at the time of the measurement |
| solar_zenith_angle | Float32 | Degrees | Solar zenith angle at the time of the measurement |
| sounding_id | Long | | From scan start time in UTC |
| source_files | | | Source L2 File Names for these soundings |
| time | Long | Seconds | Seconds since 1970-01-01 00:00:00 |

| Element | Type | Unit | Comment |
|-----------------------|---------|------|--|
| warn_level | | | Data Quality Indicator.0=Most likely good; 9=least likely good (**Note – not calculated in this version of the data product) |
| xco2 | Float32 | ppm | Column-averaged dry-air mole fraction of CO2 (Bias corrected as described in Section 2.7.3) |
| xco2_apriori | Float32 | ppm | A priori Xco2 value |
| xco2_averaging_kernel | Float32 | | Xco2 column averaging kernel |
| xco2_quality_flag | Byte | | Xco2 quality flag |
| xco2_uncertainty | Float32 | ppm | Xco2 posterior error estimate |

Table 17 Contains description of the fields in the “Preprocessor” folder of the Lite files.

| Element | Type | Unit | Comment |
|-----------------------|----------------|------|--|
| co2_ratio | Float32 | | Band 3 / Band 2 Ratio of retrieved Single-band XCO2 using IMAP-DOAS algorithm |
| dp_abp | Float32 | hPa | Retrieved-Prior Pressure from the fast O2A-band only preprocessor retrieval |
| h2o_ratio | Float32 | | H2O Ratio |
| o2_ratio_p_idp | Float32 | | O2 Ratio (nonscattering retrieval) from IMAP-DOAS algorithm, GOSAT P Polarization |
| o2_ratio_s_idp | Float32 | | O2 Ratio (nonscattering retrieval) from IMAP-DOAS algorithm, GOSAT S Polarization |
| xco2_strong_idp | Float32 | | XCO2 from Strong CO2 Band only, IMAP-DOAS algorithm |
| xco2_weak_idp | Float32 | | XCO2 from Weak CO2 Band only, IMAP-DOAS algorithm |

Table 18 Contains description of the fields in the “Retrievals” folder of the Lite files.

| Element | Type | Unit | Comment |
|----------------|---------|------|--|
| albedo_1 | float32 | | Retrieved Band 1 (0.76 micron) surface albedo |
| albedo_2 | float32 | | Retrieved Band 2 (1.6 micron) surface albedo |
| albedo_3 | float32 | | Retrieved Band 1 (2.04 micron) surface albedo |
| albedo_slope_1 | float32 | | Retrieved Band 1 albedo slope |
| albedo_slope_2 | float32 | | Retrieved Band 2 albedo slope |
| albedo_slope_3 | float32 | | Retrieved Band 3 albedo slope |
| aod_bc | float32 | | Retrieved Black Carbon Optical Depth at 0.755 microns |
| aod_dust | float32 | | Retrieved Dust Aerosol Optical Depth at 0.755 microns |
| aod_ice | float32 | | Retrieved Ice Cloud Optical Depth at 0.755 microns |
| aod_oc | float32 | | Retrieved Organic Carbon Optical Depth at 0.755 microns |
| aod_seasalt | float32 | | Retrieved Sea Salt Carbon Optical Depth at 0.755 microns |
| aod_sulfate | float32 | | Retrieved Sulfate Aerosol Optical Depth at 0.755 microns |
| aod_total | float32 | | Retrieved Total Cloud+Aerosol Optical Depth at 0.755 microns |
| aod_water | float32 | | Retrieved Water Cloud Optical Depth at 0.755 microns |

| Element | Type | Unit | Comment |
|------------------------------|---------|----------------------|--|
| b1offset | float32 | | Retrieved Band 1 (0.76 micron) radiance offset |
| co2_grad_del | float32 | | level 13 is at P/Psurf=0.631579 |
| deltaT | float32 | | Retrieved Offset to Prior Temperature Profile in Kelvin |
| diverging_steps | int8 | | No. of diverging steps taken in retrieval |
| dp | float32 | hPa | Retrieved-Prior Pressure from the L2 Full-Physics retrieval |
| fs | float32 | W / m ** 2 / sr / um | Simultaneous Fluorescence retrieval (at 757 nm) by L2 code; note this is different than the dedicated retrieval using only solar lines |
| grad_co2 | float32 | | level 13 is at P/Psurf=0.631579 |
| h2o_scale | float32 | | Retrieved scale factor to Prior Water Vapor Profile |
| iterations | int8 | | No. of iterations used in retrieval |
| lm_param | float32 | | Value of Levenberg-Marquardt Parameter on final iteration |
| logDWS | float32 | | Retrieved max(log(aod_dust+aod_sulfate+aod_ss),-5), at 0.755 microns |
| psurf | float32 | hPa | Surface pressure retrieved by the Level-2 retrieval |
| psurf_apriori | float32 | hPa | Prior surface pressure used in the retrieval, as determined by ECMWF short-term (0-9 hour) forecast |
| reduced_chi_squared_per_band | float32 | | Reduced Chi-Squared for each band (1,2,3) of L2 spectral fit |
| s31 | float32 | | Ratio of Band 3 to Band 1 signal level |
| s32 | float32 | | Ratio of Band 3 to Band 2 signal level |
| SigmaB | float32 | | Multiply Psurf by these values to get the pressure layer boundaries (= pressure levels) |
| snr_strong_clip | float32 | | Band 3 SNR clipped at 600 |
| surface_type | int8 | | Surface type used in the retrieval: 0=ocean and corresponds to a Coxmunk+Lambertian surface; 1=land and corresponds to a pure Lambertian surface |
| T700 | float32 | K | Temperature at 700 hPa (from ECMWF) |
| tcwv | float32 | kg / m ** 2 | Retrieved TCWV obtained by multiplying retrieved h2o_scale factor to prior (ECMWF) TCWV |
| tcwv_apriori | float32 | kg / m ** 2 | Prior TCWV (from ECMWF prior profile) |
| tcwv_uncertainty | float32 | kg / m ** 2 | Retrieved TCWV Posterior Uncertainty |
| windspeed | float32 | m / s | Surface wind speed retrieved by the Level-2 retrieval |
| windspeed_apriori | float32 | m / s | Surface wind speed retrieved by the Level-2 retrieval |
| xco2_raw | float32 | | Raw value of Retrieved XCO2 (not bias corrected) |

Table 19 Contains description of the fields in the “Sounding” folder of the Lite files.

| Element | Type | Unit | Comment |
|---------------|---------|------|---|
| airmass | float32 | | Airmass, computed as $1/\cos(\text{solar_zenith_angle}) + 1/\cos(\text{sensor_zenith_angle})$ |
| altitude | float32 | m | Surface Altitude in meters above sea level |
| gain | string8 | | TANSO-FTS gain mode: H is the high-gain mode (used over most of the planet); M is the medium gain mode (used over very bright surfaces) |
| glint_angle | float32 | | Angular distance from viewing along the perfect glint direction |
| l1b_type | int32 | | |
| land_fraction | int8 | | Fraction of the footprint that contains land in percent |
| path | uint8 | | GOSAT fixed orbit path number ranging from 1-45 |

| Element | Type | Unit | Comment |
|----------------------|---------|------|---|
| sensor_azimuth_angle | float32 | | azimuth angle of the satellite at the time of the measurement |
| snr_o2 | float32 | | O2A-Band Continuum Signal-to-Noise Ratio |
| snr_strong_co2 | float32 | | Strong CO2-Band Continuum Signal-to-Noise Ratio |
| snr_weak_co2 | float32 | | Weak CO2-Band Continuum Signal-to-Noise Ratio |
| solar_azimuth_angle | float32 | | solar azimuth angle at the time of the measurement |

5. Tools and Data Services

HDFView

HDFView is a Java based graphical user interface created by the HDF Group that can be used to browse all ACOS HDF products. The utility allows users to view all objects in an HDF file hierarchy, which is represented as a tree structure. HDFView can be downloaded or support found at: <http://www.hdfgroup.org/hdf-java-html/hdfview/>.

Mirador

The GES DISC provides basic temporal, advanced (event), and spatial searches through its search and download engine, Mirador (<http://mirador.gsfc.nasa.gov>). Mirador offers various download options that suit users with different preferences and different levels of technical skills. Users can start from a point where they don't know anything about these particular data, its location, size, format, etc., to quickly find what they need by just providing relevant keywords, like "ACOS", or "CO2".

Here is a direct link to the v2.9 ACOS science products on this site:

http://mirador.gsfc.nasa.gov/cgi-bin/mirador/collectionlist.pl?search=1&keyword=acos_l2s+2.9

Here are 2 methods to download the v2.9 collection:

1) Mirador Webpage

- Clicking the link above will display the collection for 2.9. Beneath the collection name, click the link "View Files"; this link will display all the files for v2.9. From here, click in the checkbox(es) to select the file(s) of interest. Click one of the buttons at the top to add the file(s) to the Cart. Doing this will update the page to show the data set collection name. On the Shopping Cart page, click the "Checkout" button. This will display the Download Data page with instructions on how to download the selected products.

2) Command-line

To build a list of ftp-paths to data files from the v2.9 collection, run the following Unix command:

```
wget "http://mirador.gsfc.nasa.gov/cgi-bin/mirador/granlist.pl?page=1&dataSet=ACOS_L2S&version=2.9&location=%28-90,-180%29,%2890,180%29&startTime=2009-03-30&endTime=2011-12-30&format=rss&maxgranules=100000" -nv -O - | sed -n '/>ftp:/ s|*</link>||gp'
```

Note the time constraints, and the version, that can be changed as appropriate. The acquired list of ftp-paths to the data files can be used in a number of ways to download the files. The most convenient would be to use “wget” from Unix command-line:

```
wget -i list_of_files.txt
```

where the list of the ftp-paths was stored in the text file “list_of_files.txt”

Global Change Master Directory

Information about GOSAT/ACOS data can be researched alongside with other relevant collections in GCMD (Global Change Master Directory):

<http://gcmd.nasa.gov/>

or

http://gcmd.gsfc.nasa.gov/getdif.htm?GES_DISC_ACOS_L2S_V2.9

6. Contact Information

Contact information of the producer of the data products:

ACOS operations team: sdosops@nephthys.jpl.nasa.gov

Contact information for interpretation and usage of the data products:

ACOS data team: acos@jpl.nasa.gov

The following list is of related organizations, web sites or publications that may be beneficial to the user.

- Japanese Aerospace Exploration Agency:
 - http://www.jaxa.jp/projects/sat/gosat/index_e.html
- Japanese National Institute for Environmental Studies:
 - http://www.gosat.nies.go.jp/index_e.html

7. Acknowledgements, References and Documentation

Acknowledgements

This research was carried out at the Jet Propulsion Laboratory, California Institute of Technology, under a contract with the National Aeronautics and Space Administration.

Figures 5 and 6 are taken from the JAXA press release “Greenhouse Gases Observing Satellite “IBUKI” (GOSAT) “First Light” Acquired by Onboard Sensors”, February 9, 2009 (JST).

Links

The following list provides references to relevant documentation that users may find helpful.

- General GOSAT information:
 - http://www.jaxa.jp/projects/sat/gosat/index_e.html
 - http://www.gosat.nies.go.jp/index_e.html
 - http://www.gosat.nies.go.jp/eng/GOSAT_pamphlet_en.pdf
- Level 2 algorithm information:
 - ACOS Level 2 Algorithm Theoretical Basis Document, JPL D-65488
- Releases and publications:
 - http://www.jaxa.jp/press/2009/02/20090209_ibuki_e.html

Algorithm and Retrievals (in time order)

- Kuze, A., Suto, H., Shiomi, K., kawakami, S., Tanaka, M., Ueda, Y., Deguchi, A., Yoshida, J., Yamamoto, Y., Kataoka, F., Taylor, T. E., and Buijs, H.: Update on GOSAT TANSO-FTS performance, operations, and data products after more than six years in space, *Atmos. Meas. Tech. Discuss.*, doi:10.5194/amt-2015-333, in review, 2016.
- Crisp, D. B. M. Fisher, C. O'Dell, C. Frankenberg, R. Basilio, H. Bosch, L. R. Brown, R. Castano, B. Connor, N. M. Deutscher, A. Eldering, D. Griffith, M. Gunson, A. Kuze, L. Mandrake, J. McDuffie, J. Messerschmidt, C. E. Miller, I. Morino, V. Natraj, J. Notholt, D. M. O'Brien, F. Oyafuso, I. Polonsky, J. Robinson, R. Salawitch, V. Sherlock, M. Smyth, H. Suto, T. E. Taylor, D. R. Thompson, P. O. Wennberg, D. Wunch and Y. L. Yung (2012), The ACOS CO₂ retrieval algorithm – Part II: Global XCO₂ data characterization, *Atmos. Meas. Tech. Discuss.*, 5, 687-707, 2012.
- O'Dell, C.W., B. Connor, H. Boesch, D. O'Brien, C. Frankenberg, R. Castano, M. Christi, D. Crisp, A. Eldering, B. Fisher, M. Gunson, J. McDuffie, G. C. Toon, P. O. Wennberg, and D. Wunch (2011), The ACOS CO₂ retrieval algorithm – Part 1: Description and validation against synthetic observations, *Atmos. Meas. Tech. Discuss.*, 4, 6097–6158, 2011.
- Taylor T.E., C. O'Dell, D.M. O'Brien, N. Kikuchi, T. Yokota, T. Nakajima, H. Ishida, D. Crisp, and T. Nakajima, Comparison of cloud screening methods applied to GOSAT near-infrared spectra, *IEEE Trans. Geosci. Rem. Sens.*, February 2011., doi: 10.1109/TGRS.2011.2160270.
- Kuze A., Hiroshi Suto, Masakatsu Nakajima, and Takashi Hamazaki, “Thermal and near infrared sensor for carbon observation Fourier-transform spectrometer on the Greenhouse Gases Observing Satellite for greenhouse gases monitoring”, *Applied Optics*, Vol. 48, No. 35, 10 December 2009

- Connor B. J., H. Boesch, G. Toon, B. Sen, C. Miller and D. Crisp (2008), Orbiting Carbon Observatory: Inverse method and prospective error analysis, *J. Geophys. Res.*, 113, D05305, doi:10.1029/2006JD008336.
- Boesch, H., G.C. Toon, B. Sen, R.A. Washenfelder, P.O. Wennberg, M. Buchwitz, R. de Beek, J.P. Burrows, D. Crisp, M. Christi, B.J. Connor, V. Natraj, and Y.L. Yung (2006), Space-based near-infrared CO₂ measurements: Testing the Orbiting Carbon Observatory retrieval algorithm and validation concept using SCIAMACHY observations over Park Falls, Wisconsin, *Journal of Geophysical Research-Atmospheres*, 111 (D23), 2006.
- Rodgers, C. (2000) Inverse Methods for Atmospheric Sounding: Theory and Practice. World Scientific Publishing Co Pte Ltd.
- Mandrake, L., C. Frankenberg, C.W. O'Dell, G. Osterman, P. Wennberg, and D. Wunch, 2013: Semi-autonomous sounding selection for OCO-2. *Atmos. Meas. Tech.*, 6, 2851-2864.
- Mandrake, L., C. O'Dell, D. Wunch, P.O. Wennberg, B. Fisher, G.B. Osterman, A. Eldering, OCO-2 Warn Level, Bias Correction and Lite File Product Description, Version 1.1, June 30, 2016.

Chlorophyll Fluorescence

- Frankenberg, C., Fisher, J., Worden, J., Badgley, G., Saatchi, S., Lee, J.-E., et al. (2011). New global observations of the terrestrial carbon cycle from GOSAT: Patterns of plant fluorescence with gross primary productivity. *Geophysical Research Letters*, 38(17), L17706.
- Frankenberg, C., O'Dell, C., Guanter, L., & McDuffie, J. (2012). Remote sensing of near-infrared chlorophyll fluorescence from space in scattering atmospheres: implications for its retrieval and interferences with atmospheric CO₂ retrievals. *Atmospheric Measurement Techniques*, 5(8), 2081–2094. doi:10.5194/amt-5-2081-2012.

Validation

Papers related to validation of the ACOS data product, plans for OCO-2 data validation or the TCCON network:

- Wunch et al., The Total Carbon Column Observing Network, *Phil. Trans. R. Soc. A*, 369, 2087–2112, doi:10.1098/rsta.2010.0240, 2011a.
- Wunch et al., A method for evaluating bias in global measurements of CO₂ total columns from Space, *Atmos. Chem. Phys. Discuss.*, 11, 20899-20946, 2011b.
- Wunch et al., Calibration of the Total Carbon Column Observing Network using aircraft profile data, *Atmospheric Measurement Techniques*, 3, 1351–1362, doi:10.5194/amt-3-1351-2010, <http://www.atmos-meas-tech.net/3/1351/2010/>, 2010.
- Messerschmidt et al., Calibration of TCCON column-averaged CO₂: the first aircraft campaign over European TCCON sites, *Atmos. Chem. Phys. Discuss.*, 11, 14 541–14 582, doi:10.5194/acpd-11-14541-2011, 2011.
- Keppel-Aleks et al., Sources of variations in total column carbon dioxide, *Atmospheric Chemistry and Physics*, 11, 3581–3593, doi:10.5194/acp-11-3581-2011, <http://www.atmos-chem-phys.net/11/3581/2011/>, 2011.

- Suto, H. and Kuze, A.: Correction of scan-speed instability of TANSO-FTS on GOSAT, Abstract A51C-0107 presented at 2010 Fall Meeting, AGU, San Francisco, Calif., 13-17 Dec., 2010.
- Deutscher et al., Total column CO₂ measurements at Darwin, Australia - site description and calibration against in situ aircraft profiles, *Atmos. Meas. Tech.*, 3, 947–958, doi:10.5194/amt-3-947-2010, 2010.
- Washenfelder et al., Carbondioxide column abundances at the Wisconsin Tall Tower site, *J. Geophys. Res.*, 111, D22305, doi:10.1029/2006JD007154, 2006.
- Lindqvist et al., Does GOSAT capture the true seasonal cycle of carbon dioxide?, *Atmos. Chem. Phys.*, 15, 13023-13040, doi:10.5194/acp-15-13023-2015, 2015.
- Kulawik et al., Consistent evaluation of GOSAT, SCIAMACHY, CarbonTracker, and MACC through comparisons to TCCON, *Atmos. Meas. Tech. Discuss.*, 8, 6217-6277, doi:10.5194/amtd-8-6217-2015, 2015.